Electronic Supplementary Material (ESI) for New Journal of Chemistry.

New Journal of Chemistry

Supporting Information

Photo-and Thermoresponsive *N*-Salicylideneaniline Derivatives: Solid-State Studies and Structural Aspects

Photo-and Thermoresponsive *N*-Salicylideneaniline Derivatives: Solid-State Studies and Structural Aspects

Siya T. Hulushe,*[a] Frederick P. Malan,[b] Eric C. Hosten,[c] Kevin A. Lobb,[a] Setshaba D. Khanye[d] and Gareth M. Watkins[a]

[a] Department of Chemistry, Rhodes University, P.O. Box 94, Makhanda 6139, South Africa

[b] Department of Chemistry, University of Pretoria, 02 Lynnwood Road, Hatfield, Pretoria, 0002, South Africa

[c] Department of Chemistry, Nelson Mandela University, Summerstrand, P.O. Box 77000, Gqeberha 6031, South Africa

[d] Faculty of Pharmacy, Rhodes University, P.O. Box 94, Makhanda 6139, South Africa

Corresponding authors

* hulushesiya@gmail.com

Table of Content

1. Mechanosyntheses and Powder X-ray Diffraction (PXRD)

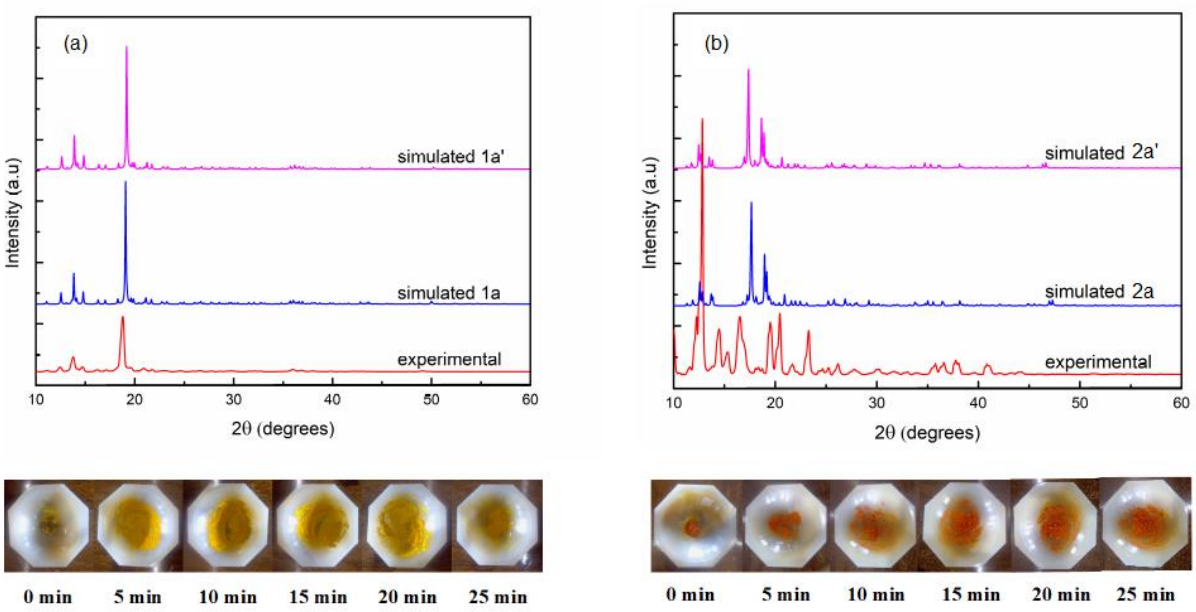

Figure S1(a). Simulated and experimental PXRD patterns (at 298 K) of (a) **1** and (b) **2** along with their respective photographs of the grinding experiments (bottom images). There are few discrepancies in (b) possibly indicating the absence of water of crystallisation as the powdered sample of compound **2** is assumed to contain no waters. The mechanochemical syntheses of **1** and **2** were carried out as follows: equimolar (1.0 mmol) amounts of 5-nitrosalicylaldehyde (yellow crystalline solid) and 2-aminophenol (dark brown crystalline powder) for **1** and *o*-anisidine (colourless liquid) for **2** were used to obtain 2-((*E*)-(2-hydroxyphenylimino)methyl)-4-nitrophenol and 2-((*E*)-(2-methoxyphenylimino)methyl)-4-nitrophenol, respectively. Neat grinding (NG) in an agate mortar lead to the formation of a yellow sample and an orange moist paste which then started to solidify after 5 minutes in the case of compound **2** and were respectively obtained in 70% and 68% yields.

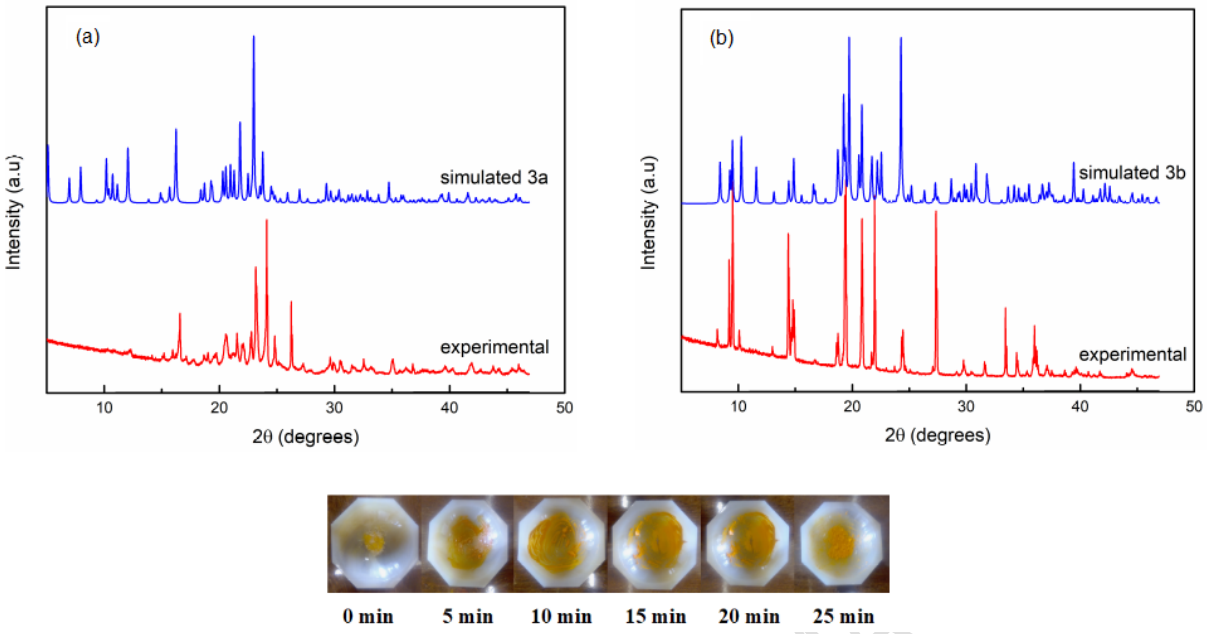

Figure S1(b). Simulated and experimental PXRD patterns (at 298 K) of (a) **3a** and (b) **3b** along with photographs of the grinding experiments (bottom image) for compound **3**. There are few discrepancies in (a) possibly indicating some impurities present or the presence of ethyl acetate as solvent of crystallisation. The mechanochemical synthesis of compound **3** was carried out as follows: equimolar (1.0 mmol) amounts of 5-nitrosalicylaldehyde (yellow crystalline solid) and 2-bromoaniline (colourless crystals) were used in order to obtain 2-((*E*)-(2-bromophenylimino)methyl)-4-nitrophenol. Neat grinding (NG) in an agate mortar lead an orange moist paste which then started to solidify after 10 minutes and the orange crystalline solid was obtained in 67% yields.

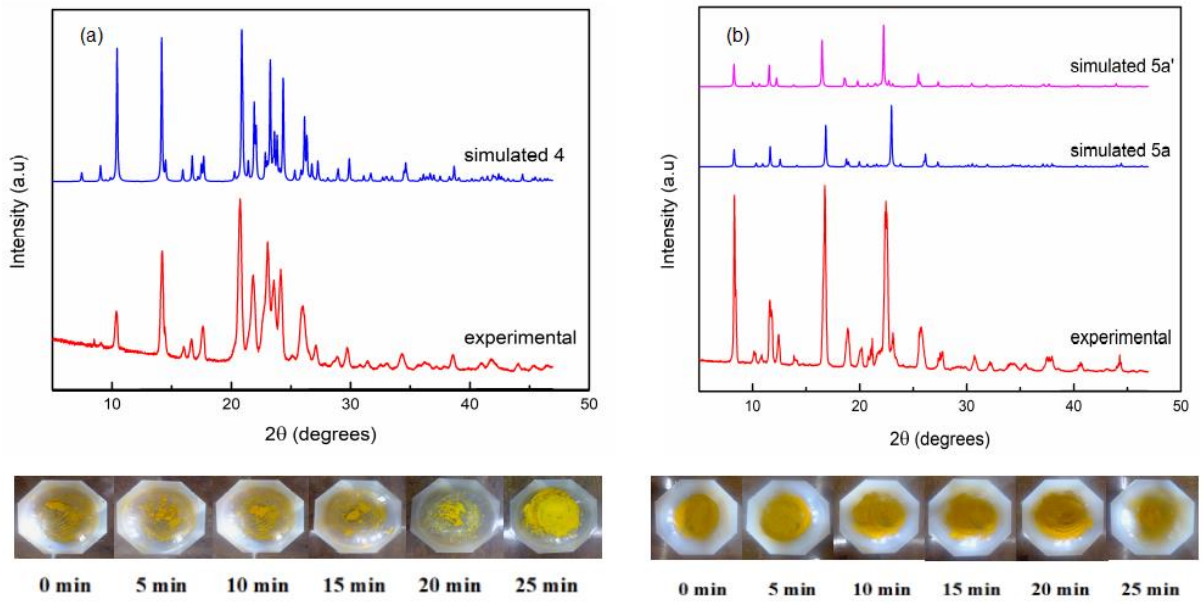

Figure S1(c). Simulated and experimental PXRD patterns (at 298 K) of (a) **4** and (b) **5** along with their photographs of the grinding experiments (bottom image) for both compounds. The mechanochemical syntheses of **4** and **5** were carried out as follows: equimolar (1.0 mmol) amounts of 5-nitrosalicylaldehyde (yellow crystalline solid) and 3-chloroaniline for **4** and 3-trifluoromethylaniline (both colourless liquids) for **5** were used to obtain 2-((*E*)-(3-chlorophenylimino)methyl)-4-nitrophenol and 2-((*E*)-(3-(trifluoromethyl)phenylimino)methyl)-4-nitrophenol, respectively. Neat grinding (NG) in an agate mortar lead to the formation of a yellow moist paste (started to solidify after 20 minutes in the case of compound **4**) and orange-yellow powdered product of compound **5** and were obtained in 61% and 59% yields, respectively.

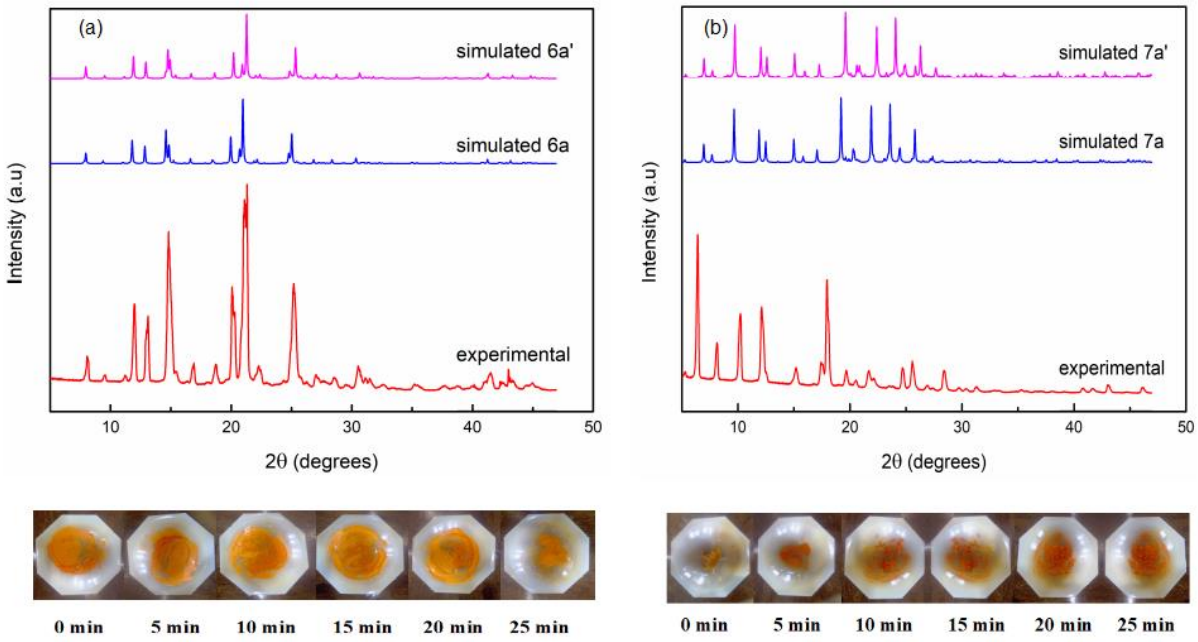

Figure S1(d). Simulated and experimental PXRD patterns (at 298 K) of (a) **6** and (b) **7** along with their photographs of the grinding experiments (bottom image) for both compounds. The mechanochemical syntheses of **6** and **7** were carried out as follows: equimolar (1.0 mmol) amounts of 5-nitrosalicylaldehyde (yellow crystalline solid) and *p*-toluidine (dark purple solid) for **6** and *p*-anisidine (purple crystalline powder) for **7** were used to obtain 2-((E)-(*p*-tolylimino)methyl)-4-nitrophenol and 2-((*E*)-(4-methoxyphenylimino)methyl)-4-nitrophenol, respectively. Neat grinding (NG) in an agate mortar lead to the formation of a yellow sample and an orange moist paste which then started to solidify after 5 minutes in the case of compound **7** and were respectively obtained in 63% and 57% yields.

2. Electron Difference Maps

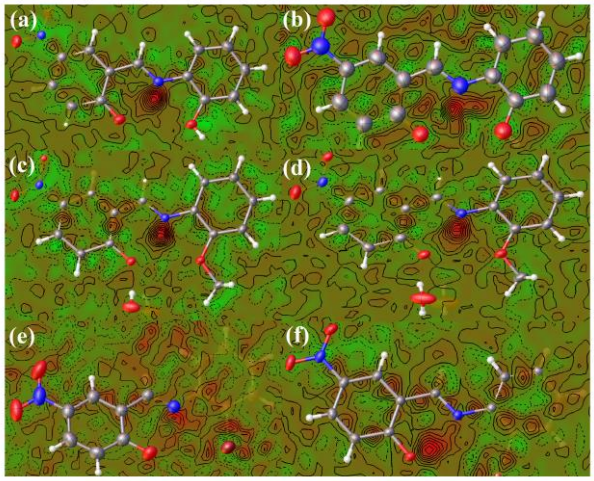

Figure S2. Electron difference maps showing the location of the H1 atom involved in intramolecular hydrogen bond in compounds (a) **1_LT**; (b) **1_RT**; (c) **2_LT**; (d) **2_RT**; (e) **3a_RT** and (f) **3b_LT**. Hydrogen atoms are shown as off-white spheres with 0.2 Å radius.

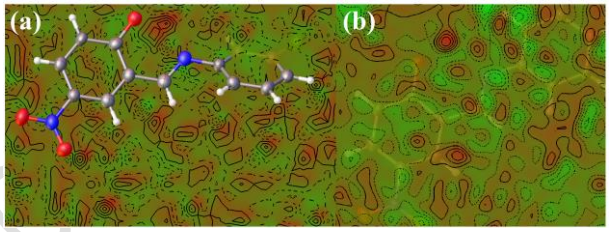

Figure S3. Electron difference maps showing the location of the H1 atom involved in intramolecular hydrogen bond in compounds (a) **4_LT** and (b) **5_RT**. Hydrogen atoms are shown as off-white spheres with 0.2 Å radius.

The location of the hydrogen atoms at either the nitrogen or oxygen atoms were determined both from electron density map and, the **KA** (d(N1–H1)) and **EI** (d(O1–H1)) bond lengths along with strong intramolecular hydrogen bonds between O1 and N1 atoms with their respective O···H/N···H bond distances are discussed. The molecular conformation in all the structures is described by the relative orientation of the torsion angles: **Tα** [∠C1–N1–C21–C26] and **Tβ** [∠N1–C1–C11–C12] (**Scheme S1**). Generally, the torsion angle in both tautomeric forms is defined by the ∠N1–H1···O1 and ∠N1···H1–O1 angles which force the fragment to adopt planarity usually with a value close to zero degrees. The dihedral angle (**ϕ**) between the aromatic ring units, packing indices, and the **ϕ** value related to the solid-state thermo- and photochromic processes of all the compounds are presented.

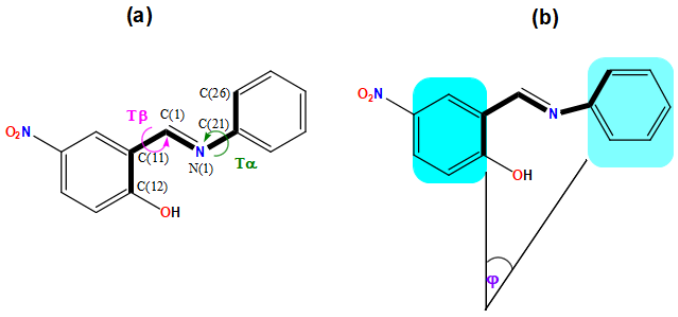

Scheme S1. (a) Definition of the **Tα** (∠C1–N1–C21–C26: green) and **Tβ** (∠N1–C1–C11–C12: magenta) torsion angles in the *N*-salicylideneaniline derivatives; (b) The **ϕ** dihedral angle formed by the two six-membered (highlighted blue regions) rings.

Table S1: Selected geometric parameters of hydrogen bonds and, graph-set assignments exhibited by intra-and intermolecular interactions (calculated using Platon[1]) in compounds **1**–**2**.

D-H···*A*	d(D-H) / (Å)	d(H···A) /(Å)	d(D-A) / (Å)	∠(D-H···*A*) /º	Graph-set motifs
1_LT					
N1–H1···O4^{i}	0.8800(1)	2.183(1)	2.596(1)	108.2(1)	
N1–H1···O1^{i}	0.8800(1)	1.896(1)	2.607(1)	136.6(1)	$S_1^1(6)$
C1–H1A···O3^{ii}	0.9499(2)	2.314(2)	3.197(2)	154.5(1)	$R_2^2(10)$
C16–H16···O3^{ii}	0.9500(2)	2.564(2)	3.384(2)	144.7(1)	$R_2^2(14)$
O4–H4···H1^{iii}	0.8570(2)	1.725(2)	2.565(1)	165.6(2)	$R_2^2(18)$
C25–H25···O2^{iv}	0.9500(2)	2.592(2)	3.201(2)	122.2(1)	–
1_RT					
N1–H1···O1^{i}	0.860(6)	1.907(6)	2.601(6)	136.8(5)	$S_1^1(6)$
C1–H1A···O3^{ii}	0.9297(7)	2.334(6)	3.202(6)	155.2(5)	$R_2^2(10)$
C16–H16···O3^{ii}	0.9310(7)	2.576(6)	3.376(6)	144.4(5)	$R_2^2(14)$
O4–H4···H1^{iii}	0.8304(5)	1.800(4)	2.576(5)	158.0(3)	$R_2^2(18)$
C25–H25···O2^{v}	0.9310(7)	2.583(6)	3.180(6)	122.4(5)	–
2_LT					
N1–H1···O4^{i}	0.8799(2)	2.136(2)	2.570(2)	109.7(1)	$S_1^1(6)$
N1–H1···O1^{i}	0.8799(2)	1.815(2)	2.556(2)	140.6(2)	$S_1^1(6)$
O5W–H5WA···O1^{i}	0.8700(3)	2.020(3)	2.887(2)	177.0(3)	$R_2^4(8)$
O6W–H6WA···O1^{i}	0.8700(4)	2.000(5)	2.865(2)	175.0(5)	$R_2^4(8)$
C1–H1A···O5W^{vi}	0.9500(2)	2.564(2)	3.288(2)	133.2(2)	–
C16–H16···O6W^{vii}	0.9500(2)	2.530(2)	3.254(2)	133.1(2)	–
C23–H23···O2^{viii}	0.9500(2)	2.381(2)	3.329(2)	175.2(2)	–
O6W–H6WA···Cg(1)^{i}	0.8698(2)	2.867(6)	3.661(1)	152.5(6)	–
C27–H27A···O3^{vi}	0.9800(5)	2.653(4)	3.591(2)	160.3(6)	$R_2^2(24)$
2_RT					
N1–H1···O4^{i}	0.8600(2)	2.149(2)	2.574(2)	110.1(1)	$S_1^1(6)$
N1–H1···O1^{i}	0.8600(2)	1.833(2)	2.559(2)	140.9(2)	$S_1^1(6)$
O5W–H5WA···O1^{i}	0.8399(4)	2.060(4)	2.873(2)	163.0(5)	$R_2^4(8)$
O5W–H5WB···O1^{ix}	0.8601(4)	2.100(5)	2.873(2)	151.0(7)	$R_2^4(8)$

Table S1: (continues...) Selected geometric parameters of hydrogen bonds and, graph-set assignments exhibited by intra-and intermolecular interactions (calculated using Platon[1]) in compounds **3**–**5**.

D-H···*A*	d(D-H) / (Å)	d(H···A) /(Å)	d(D-A) / (Å)	∠(D-H···*A*) /º	Graph-set motifs
3a_RT					
O1–H1···N1^{i}	0.8399(1)	1.858(1)	2.603(2)	147.0(1)	$S_1^1(6)$
C26–H26···O3^{x}	0.9300(2)	2.466(2)	3.250(2)	142.0(2)	$R_2^2(9)$
C1–H1A···O2^{x}	0.9300(2)	2.668(2)	3.521(2)	149.8(1)	$R_2^2(9)$
3b_LT					
N1–H1···O1^{i}	0.8600(2)	1.916(2)	2.608(2)	136.5(2)	$S_1^1(6)$
N1–H1···Br1^{i}	0.8600(2)	2.586(2)	3.040(2)	114.1(2)	$S_1^1(5)$
C26–H26···O3^{x}	0.9300(3)	2.481(3)	3.273(3)	143.2(2)	$R_2^2(9)$
C1–H1A···O2^{x}	0.9300(3)	2.715(3)	3.557(3)	150.8(3)	$R_2^2(9)$
4_LT					
O1–H1···N1^{i}	0.8340(2)	1.835(2)	2.601(3)	151.9(4)	$S_1^1(6)$
C16–H16···O3^{xii}	0.9500(1)	2.460(7)	3.329(5)	152.0(1)	$R_2^2(10)$
C22–H22···O3^{xiii}	0.9500(3)	2.679(2)	3.564(2)	155.3(7)	
4_RT					
O1–H1···N1^{i}	0.8200(2)	1.874(3)	2.605(2)	147.9(5)	$S_1^1(6)$
C16–H16··O3^{i}	0.9300(4)	2.510(1)	3.364(5)	152.6(1)	$R_2^2(10)$
C22–H22···O3^{xiv}	0.9300(1)	2.635(4)	3.553(8)	169.3(8)	
5_LT					
O1–H1···N1^{i}	0.9001(4)	1.786(0)	2.614(2)	151.1(4)	$S_1^1(6)$
C1–H1A···O3^{xvi}	0.9500(3)	2.414(3)	3.297(3)	154.6(2)	$R_2^2(14)$
C16–H16···O3^{xvi}	0.9499(3)	2.583(3)	3.427(3)	148.2(2)	$R_2^2(10)$
5_RT					
O1–H1···N1^{i}	0.8100(4)	1.890(4)	2.616(3)	150.0(4)	$S_1^1(6)$
C1–H1A···O3^{xvi}	0.9300(3)	2.440(1)	3.317(4)	157.0(0)	$R_2^2(14)$
C16–H16···O3^{xvi}	0.9500(3)	2.583(1)	3.427(0)	148.2(1)	$R_2^2(10)$

Table S1 (continue). Selected geometric parameters of hydrogen bonds and, graph-set assignments exhibited by intra-and intermolecular interactions (calculated using Platon[1]) in compounds **6**–**7**.

D-H···*A*	d(D-H) / (Å)	d(H···A) /(Å)	d(D-A) / (Å)	∠(D-H···*A*) /º	Graph-set motifs
6_LT					
N1–H1···O1^{i}	0.9400(3)	1.915(6)	2.558(1)	155.2(3)	$S_1^1(6)$
O1–H1···N1^{i}	0.7750(6)	1.671(3)	2.558(1)	140.1(6)	$S_1^1(6)$
C16–H16···O3^{xix}	0.9500(2)	2.568(2)	3.340(2)	138.6(1)	$R_2^2(10)$
C1–H1A···O3^{xix}	0.9500(2)	2.664(2)	3.376(2)	132.1(1)	$R_2^2(14)$
C26–H26···O1^{xx}	0.9500(2)	2.664(1)	3.567(1)	158.8(1)	–
C27–H27B···O3^{xxi}	0.9800(7)	2.692(5)	3.633(2)	161.0(5)	–
C27–H27C···O2^{xxii}	0.9800(6)	2.630(4)	3.394(2)	135.0(5)	–
6_RT					
N1–H1···O1^{i}	1.3910(4)	1.260(4)	2.559(2)	149.8(4)	$S_1^1(6)$
O1–H1···N1^{i}	1.2600(4)	1.391(4)	2.559(2)	149.8(4)	$S_1^1(6)$
C16–H16···O3^{xix}	0.9300(2)	2.617(2)	3.374(2)	139.0(1)	$R_2^2(10)$
C1–H1A···O3^{xix}	0.9300(2)	2.707(2)	3.408(2)	132.8(1)	$R_2^2(14)$
C22–H22···O1^{xx}	0.9300(2)	2.714(2)	3.597(2)	158.9(1)	–
C27–H27C···O2^{xxii}	0.9600(7)	2.677(5)	3.418(3)	134.4(7)	$R_2^2(18)$
7_LT					
N1–H1···O1^{i}	1.4543(4)	1.158(4)	2.545(4)	153.8(3)	$S_1^1(6)$
C27–H27B ···O2^{xxv}	0.9810(7)	2.555(9)	3.279(3)	130.5(6)	–
C14–H14···O4^{xxvi}	0.9500(3)	2.563(2)	3.451(2)	155.6(2)	$R_2^2(8)$
C1–H1A···O3^{xxvii}	0.9500(3)	2.431(2)	3.283(2)	149.1(2)	$R_2^2(14)$
C16–H16···O3^{xxviii}	0.9500(3)	2.583(2)	3.401(3)	144.6(2)	$R_2^2(10)$
7_RT					
N1–H1···O1^{i}	1.4590(2)	1.1504(2)	2.558(1)	156.2(2)	$S_1^1(6)$
C27–H27B ···O2^{iv}	0.9600(4)	2.606(6)	3.510(1)	132.5(4)	–
C14–H14···O4^{xxix}	0.9300(2)	2.640(1)	3.330(2)	156.0(1)	$R_2^2(8)$
C16–H16···O3^{xxviii}	0.9300(2)	2.631(1)	3.433(1)	144.7(1)	$R_2^2(10)$
C1–H1A···O3^{xxviii}	0.9301(2)	2.454(2)	3.296(2)	150.5(1)	$R_2^2(14)$

Symmetry codes: (i) x, y, z; (ii) 2-x, 1-y,1-z; (iii) -x, 1-y, 2-z; (iv) 3/2-x, -1/2+y, 3/2-z; (v) 3/2-x, 1/2+y, 3/2-z; (vi) 1-x, 1-y, 1-z; (vii) 1-x, -y, 1-z; (viii) 1/2+x, 1/2+y, z; (ix) 1-x, y, 1/2-z; (x) 1-x, -1/2+y, 1/2-z; (xi) 2-x, -1/2+y, 3/2-z; (xii) 1-x, 1-y, -z; (xiii) 2-x, 1-y, -z; (xiv) 2-x, 2-y, 1-z; (xv) 1-x, 2-y, 1-z; (xvi) 1-x, y, 1-z; (xvii) x, y, 1+z; (xviii) 2-x, y, 1-z; (xix) 1-x, 1-y, 2-z; (xx) x, y, -1+z; (xxi) -1+x, y, z; (xxii) -1+x, y, -1+z; (xxiii) x, 3/2-y, -1/2+z; (xxiv) x, 3/2-y, 1/2+z; (xxv) 1/2-x, 1/2+y, 1/2-z; (xxvi) 3/2-x, -1/2+y, 1/2-z; (xxvii) -x, 1-y, -z; (xxviii) 2-x, 1-y, 2-z.

Table S2: Selected bond lengths, torsion angles of (∠N1–C1–C11), (**Tα**: [∠C1–N1–C21–C26] and **Tβ**: [∠N1–C1–C11–C12]) units, dihedral angles (**ϕ**) between the planes of the terminal phenyl rings (calculated using Mercury[2]) and packing indices of the molecules (calculated using Platon[1]).

Compound	C1–N1 [Å]	C12–O1 [Å]	∠Tor. [°]	Tα [°]	Tβ [°]	ϕ [°]	PI[b] [%]
1_LT	1.288(7)	1.267(7)	124.5(5)	-0.50(8)	-1.20(8)	2.34(4)	69.99
1_RT	1.300(2)	1.273(4)	122.8(1)	0.27(2)	2.08(2)	2.26(3)	69.89
2_LT	1.306(2)	1.284(2)	120.6(1)	0.10(2)	0.20(2)	1.45(1)	71.14
2_RT	1.300(2)	1.282(2)	120.9(1)	0.89(2)	-0.09(2)	1.82(1)	72.40
3b_LT	1.281(2)	1.335(2)	120.9(1)	-12.4(2)	3.1(2)	8.22(9)	71.67
3a_RT	1.268(3)	1.332(3)	121.7(2)	11.4(3)	-2.6(3)	8.31(9)	69.13
4 _LT	1.281(3)	1.336(4)	121.4(3)	40.5(4)	1.4(5)	42.5(1)	72.47
4 _RT	1.281(2)	1.333(2)	121.3(2)	-40.3(2)	-0.6(3)	41.7(6)	73.07
5_LT	1.282(3)	1.340(3)	121.1(1)	0.00(1)	-0.00(1)	0.00(1)	71.12
5_RT	1.276(3)	1.332(3)	121.5(2)	0.00(1)	0.00(1)	0.00(1)	-
6_LT	1.290(2)	1.319(1)	120.2(1)	35.3(2)	4.9(2)	42.6(8)	68.84
6_RT	1.289(2)	1.321(2)	120.3(1)	-30.6(2)	-5.0(2)	42.5(7)	67.38
7_LT	1.288(2)	1.330(2)	120.4(2)	-4.70(3)	1.3(3)	3.15(1)	70.52
7_RT	1.286(1)	1.319(1)	120.9(1)	4.41(2)	-0.95(2)	3.29(2)	70.30

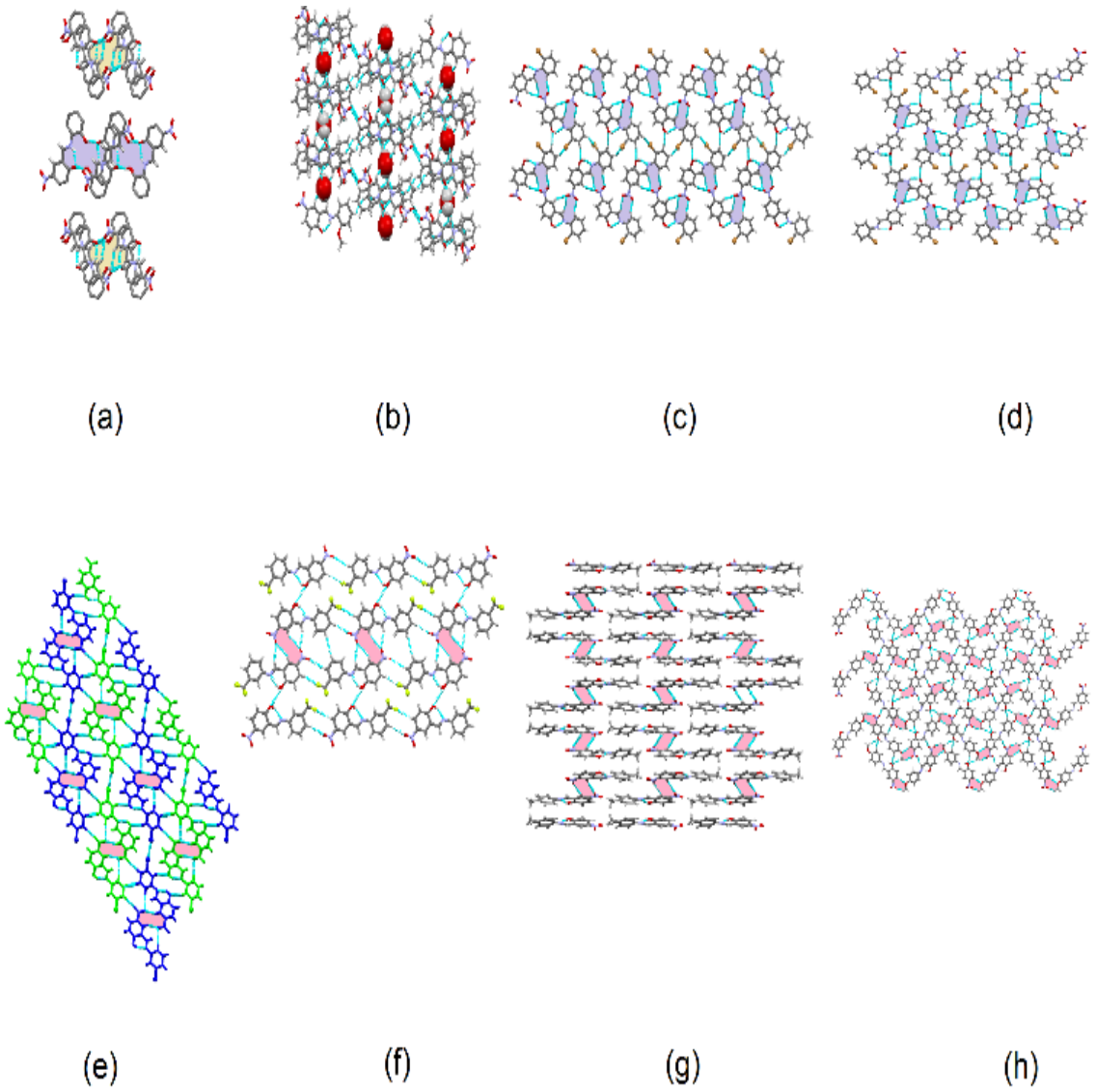

Figure S4. The packing patterns of (a) **1_LT** (along the *c*-axis), (b) **2_LT** (along the *b*-axis), (c) **3a_RT**, (d) **3b_LT**, (e) **4_LT** (all viewed along the *a*-axis), (f) **5_LT** (along the *b*-axis), (g) **6_LT** (along the *c*-axis) and (h) **7_LT** (viewed along the *a*-axis).

Crystal Packing Features: In an attempt to understand supramolecular interactions, we also discuss hydrogen bonding interactions and crystal packing features of the compounds. However, we only discussed packing features for one structure in cases where a crystal gave the same structure solution at both temperatures (LT and RT). Strong intramolecular hydrogen bonds occur between the O1 and N1 atoms, with respective O1···H1 bond lengths of 1.896(1), 1.907(6), 1.815(1), 1.833(1) and 1.916(2) Å, while their respective N1···O1 distances are 2.607(1), 2.601(6), 2.556(1), 2.559(1) and 2.608(2) Å; the values for the ∠O1···H1–N1 angles are 136.56(1), 136.80(5), 140.60(1), 140.90(1) and 136.51(2)°, respectively, with compound **3a_RT** possessing the shortest bond angle. In **1_LT**, the phenolic oxygen atom O4 in the molecule at (x, y, z) acts as a hydrogen bond donor to the phenolate oxygen atom O1 at (-x, 1-y, 2-z) while the nitro group oxygen atom O3 serves as hydrogen bond acceptor to both the phenyl ring carbon C16 and carbon atom C1 at (2-x, 1-y, 1-z). The propagation of dimers *via* intermolecular O4–H4···O1 (1.725(2) Å), C16–H16···O3 (2.564(2) Å) and, C1–H1A···O3 (2.314(2) Å) together with strong intramolecular N1–H1···O1 (1.898(1) Å) hydrogen bonds in **1_LT** generate [Etter's symbols: $R_2^2(18)$, $R_2^2(14)$ and, $R_2^2(10)$ and $R_2^2(6)$, respectively] motifs to which their combined effect form a polymeric chain running along the [1 0 ½] direction (Figure S4). Moreover, packing in **1_LT** is stabilized through weak C25–H25···O2 (at 3/2-x, -1/2+y, 3/2-z with 2.592(2) Å distance) intermolecular hydrogen bonding as well as Cg(1)···Cg(2) [Cg(1): C11–C16, Cg(2): C21–C26] stacking interactions with symmetry code (1-x, 1-y, 2-z) between the phenyl rings (centroid–centroid distance of 3.345 Å), Cg(1)···π(arene) involving O3 at (-1+x, y, z), 2x Cg(2)···π(arene) [facilitated by respective O2 and O3 at (1-x, 1-y, 1-z) and (3/2-x, -1/2+y, 3/2-z)], π(lone-pair: lp)···π(lp) [between the phenolate O1 and O4 at (-x, 1-y, 2-z)] and π(arene)···π(lp) [between C1 and O3 at (2-x, 1-y, 1-z)] separated by a stacking distances of 3.127(1), 3.189(1) and 3.418(2), 2.565(1) and 3.197(1) Å, respectively.

In the presence of crystal water, hydrogen bonded layers are formed in **2_LT**, including molecular pairs related by a centre of symmetry with O5W–H5WA···O1 (2.020(3) Å), O6W–H6WA···O1 (2.000(5) Å) [which generate bifurcated $\boldsymbol{R_2^2}(8)$ graph set motifs] and C1–H1A···O5W (2.564(2) Å) hydrogen bonds. Furthermore, the water oxygen atom O6W acts as a hydrogen bond acceptor to the phenyl ring carbon C16 at (1-x, -y, 1-z), the nitro group oxygen atom O2 serves as hydrogen bond acceptor to another phenyl ring carbon C23 at (-1/2+x, -1/2+y, z) and their combination forms polymeric *zig-zag* chains propagating along the *ab*-plane while N1–H1···O1 at (1-x, 1-y, 1-z) forms intramolecular hydrogen bonds [generating $\boldsymbol{S_1^1}(6)$ synthon] with supramolecular distances of 2.530(2), 2.381(2) and 1.815(2) Å, respectively. The crystal water molecules propagating parallel to *b*-axis further link 2D layers into a 3D hydrogen-bonded chains running along the *ac*-plane. Besides the noticeable hydrogen bonds, there exist Cg(1)···Cg(2) [centroid–centroid distance of 4.357(9) Å] at (1-x, -y, 1-z) stacking interactions in **2_LT**.

We also observed π(lp)···π(lp) between oxygen atoms O1···O5W and O1···O6W both at (x, y, z), Cg(1)···π(arene) at (1-x, -y, 1-z), O6W–H6WA···Cg(1) at (x, y, z), C27–H27A···O3 at (1-x, 1-y, 1-z) and D–A short H14···H24 at (-1/2+x, 1/2-y, -1/2+z) interatomic interactions set-apart by stacking/supramolecular distances of 2.887(0), 2.865(0), 3.374(2), 2.867(6), 2.653(4) and 2.287(2) Å, respectively. The propagation of the uncommon bifurcated $\boldsymbol{R_2^2}(9)$ graph set mediated *via* strong C26–H26···O3 (2.481(3) Å) and weak C1–H1A···O2 (2.715(3) Å) both at (1-x, -1/2+y, 1/2-z) intermolecular hydrogen bonds exist in **3a** while weak C16–H16···O2 (2.659(3) Å) at (1-x, -1/2+y,

1/2-z) and C23–H23···O1 (2.703(3) Å) at (2-x, -1/2+y, 3/2-z) hydrogen bonds are defined with the latter forming $C_1^2(6)$ polymeric chains running along the *b*-axis. Furthermore, compound **3a_RT** possess a rare $S_1^1(5)$ graph set motif *via* strong N1–H1···Br1 (2.586(2) Å) at (x, y, z) intramolecular hydrogen bonding. It is worth to note that **3b_LT** displays same graph motifs and intermolecular hydrogen bonds [C26–H26···O3 (2.466(2) Å), C1–H1A···O2 (2.668(2) Å) both at (1-x, -1/2+y, 1/2-z), C16–H16···O2 (2.604(2) Å) at (1-x,-1/2+y, 1/2-z) and C23–H23···O1 (2.659(2) Å) at (2-x, -1/2+y, 3/2-z)] described for compound **3a_RT**. Moreover, like in **3a_RT**, the **3b_LT** tautomeric form exhibit extra C22–Br1···Cg(1) (3.946(8) Å) at (-x, -1/2+y, 1/2-z) and C24–H24···Br1 (3.017(8) Å) at (-x, -1/2+y, 1/2-z) halogen interactions including Cg(1)···Cg(2) and Cg(2)···Cg(1) [centroid–centroid distances of 3.872(9) and 3.884(9) Å, respectively] at (1-x, 1-y, 1-z) and (2-x, 1-y, 1-z), π(lp)···π(lp) [between carbon atoms C1] at (1-x, 1-y, 1-z) and π(lp)···π(lp) [between oxygen atoms O1 and O2] at (x, 1/2-y, -1/2+z) stacking interactions with distances of 3.355(2) and 3.019(2) Å respectively.

In the crystal of **4_LT**, chains of molecules are formed along the *b*-axis by two-point intermolecular C16–H16···O3 (2.460(2) Å) at (1-x, 2-y, 1-z) hydrogen bonds resulting in $R_2^2(10)$ fused motif. Likewise, the interaction of adjacent chains mediated *via* C24–H24··O2 (2.626(1) Å) at (-1/2+x, 1/2-y, 1/2+z), C26–H26···O3 (2.561(1) Å) at (1-x, 1-y, 1-z), C22–H22···O1 (2.679(5) Å) at (1/2-x, -1/2+y, 1/2-z) hydrogen bonds and Cl1···Cl1 halogen-halogen bonding (3.288(4) Å) at (1-x, 1-y, -z) results in the formation of a 3D supramolecular network.

Similarly, with the previously discussed structures, the quinoid ring system or $S_1^1(6)$ graph symbol in **5_LT**, is generated by strong intramolecular O1–H1···N1 (1.786(4) Å) hydrogen bonding. Moreover, centrosymmetric dimers running along the *a*-axis, which in turn construct Etter's symbol $R_2^2(14)$, are generated by two-point intermolecular C1–H1A···O3 (2.414(3) Å) at (1-x, y, 1-z) hydrogen bonds. The crystal of **5_LT** is further stabilized through hydrogen bonding C24–H24···O2 (2.561(2) Å) at (x, y, -1+z) and C14–H14···F1 (2.568(2) Å) at (x, y, -1+z) intermolecular forces to form polymeric chains projected along the *b*-axis. There also exist Cg(1)···Cg(1) and Cg(1)···Cg(2) at (1/2-x, -1/2+y, 1-z) and (1/2-x, 1/2-y, 1-z) [with respective centroid–centroid distances of 3.660(1) and 3.576(1) Å] stacking interactions between the phenyl rings, F1···F2 at (x, y, 2-z) [with interatomic distances of 3.098(2) Å] type II halogen–halogen bonding, π(lp)···π(lp) involving two O1 oxygen atoms at (-x, y, 1-z) and D–A short H25···H25 at (1-x, y, 2-z) interatomic interactions separated by intermolecular distances of 3.002(1) and 3.350(2), respectively.

In the crystal of **6_LT**, chains of molecules are formed along the *c*-axis by two-point intermolecular C16–H16···O3 (2.538(1) Å) at (1-x, 1-y, 2-z) hydrogen bonds resulting in $R_2^2(10)$ fused motif. Likewise, the interaction of adjacent chains mediated *via* C1–H1A···O3 (2.664(2) Å) at (1-x, 1-y, 2-z), C26–H26···O1 (2.664(1) Å) at (x, y, -1+z), C27–H27B···O3 (2.692(5) Å) at (-1+x, y, z) and C27–H27C···O2 (2.630(4) Å) at (-1+x, y, -1+z) hydrogen bonds results in the formation of 2D supramolecular architectures observed in **AYUGUX** and **AYUGUX01**.

Essentially, compound **7_LT** displays numerous contacts which give rise to a cyclic dimer mediated by strong intermolecular C27–H27B···O2 (2.555(9) Å) at (1/2-x, 1/2+y, 1/2-z) while C14–H14···O4 (2.563(2) Å) at (3/2-x, -1/2+y, 1/2-z), C1–H1A···O3 (2.431(2) Å) at (-x, 1-y, -z), C16–H16···O3 (2.583(2) Å) at (-x, 1-y, -z), C27–H27C···O1 (2.548(9) Å) at (1-x, 1-y, 1-z) and C25–H25···O1 (2.516(2) Å) at (2-x, 1-y, 1-z) hydrogen bonds generate $R_2^2(8)$,

$R_2^2(14)$, $R_2^2(10)$, $R_2^2(18)$ and $R_2^2(24)$ ring motifs, like in the **MOSLUC** structure, to form a polymeric 2D supramolecular network propagating along the *a*-axis. Additionally, packing in **7_LT** is locked *via* Cg(1)···Cg(1) at (1+x, y, z) and Cg(2)···Cg(2) at (-1+x, y, z) stacking interactions with 3.8168(13) and 3.8170(13) Å centroid–centroid distances, respectively, C27–H27A···π (2.851(4) Å) at (-1+x, y, z), Cg(2)···π(lp) (3.194(3) Å) attractive dipole–dipole interaction forces mediated by O2 at (3/2-x, -1/2+y, 1/2-z) and D–A short H26···H26 (2.300(3) Å) intermolecular contacts at (2-x, 1-y, 1-z).

3. Thermochromic Compounds

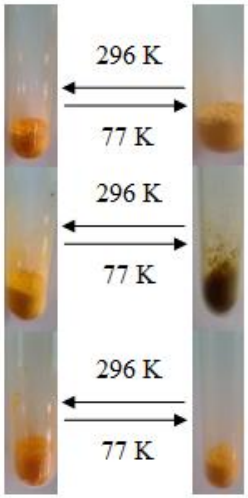

Figure S5. Photograph images of thermochromic compounds **3b** (top), **4** (middle) and **5** (bottom) at 77 K and 298 K.

4. Variable Temperature Single-Crystal X-ray Diffraction Studies

Table S3: Structural data (collection at **LT**) and refinement parameters for compounds **1**–**7**.

Compound	1_LT	2_LT	3b_LT	4_LT	5_LT	6_LT	7_LT
Empirical Formula	$C_{13}H_{10}N_2O_4$	$C_{14}H_{14}N_2O_6$	$C_{13}H_9N_2O_3Br$	$C_{13}H_9N_2O_3Cl$	$C_{14}H_9N_2O_3F_3$	$C_{14}H_{12}N_2O_3$	$C_{14}H_{12}N_2O_4$
M. W. (g.mol^{-1})	258.24	306.29	321.13	275.66	310.23	256.26	272.26
T (K)	150	150	150	150	150	150	150
λ (Å)	1.54178	0.71073	0.71073	1.54178	0.71073	0.71073	0.71073
Crystal habit, colour	plate, orange	prism, red-orange	block, orange	needle, yellow	rod, orange	needle, orange	needle, yellow
Crystal size (mm^3)	0.781 x 0.279 x 0.116	0.345 x 0.181 x 0.167	0.533 x 0.264 x 0.222	0.256 x 0.137 x 0.073	0.331 x 0.304 x 0.283	0.260 x 0.219 x 0.084	0.221 x 0.092 x 0.033
Lattice	Monoclinic	Monoclinic	Monoclinic	Monoclinic	Monoclinic	Monoclinic	Monoclinic
Space group	$P2_1/n$	$C2/c$	$P2_1/c$	$P2_1/n$	$C2/m$	$P2_1/c$	$P2_1/n$
a (Å)	6.2847(10)	26.0543(14)	7.4282(9)	14.6564(3)	14.331(3)	14.0746(8)	3.8169(5)
b (Å)	23.555(3)	6.9252(4)	11.5053(14)	3.7374(1)	6.5948(14)	13.9715(7)	21.416(3)
c (Å)	7.7504(12)	15.7729(9)	14.0071(16)	21.4431(4)	14.147(3)	6.1944(4)	15.220(3)
β (°)	94.788(9)	111.788(2)	93.651(6)	92.109(2)	107.308(6)	95.289(2)	96.042(5)
Vol (Å^3)	1143.3(3)	2642.6(3)	1194.7(2)	1173.8(5)	1276.5(4)	1212.90(12)	1237.2(3)
Z	4	8	4	4	4	4	4
D_{calcd} (g.cm^{-3})	1.500	1.459	1.785	1.560	1.641	1.403	1.4615
F(000)	536.0	1216	639.2	564.0	632.5	536	568.3
μ (mm^{-1})	0.958	0.112	3.446	2.955	0.143	0.100	0.109
No. reflns	36114	34814	37547	11919	46865	5853	84574
Data / restr. / par.	2226 / 0 / 172	1870 / 0 / 202	2964 / 0 / 175	2249 / 0 / 176	1412 / 0 / 132	1474 / 0 / 179	2490 / 0 / 186
R(int) / R(sigma)	0.2513 / 0.0988	0.1147 / 0.0328	0.0314 / 0.0133	0.0556 / 0.0308	0.0423 / 0.0098	0.0655 / 0.0533	0.0622 / 0.0143
R_1 / wR_2 ($I > 2\sigma(I)$)[a]	0.0974 / 0.2320	0.0607 / 0.1506	0.0203 / 0.0491	0.0437 / 0.1234	0.0335 / 0.0870	0.0622 / 0.1566	0.0407 / 0.0996
R_1 / wR_2 [all data]	0.1983 / 0.2890	0.1179 / 0.2317	0.0242 / 0.0518	0.0468/ 0.1264	0.0438 / 0.1062	0.1151 / 0.2187	0.0616 / 0.1330
GOOF	1.029	1.022	1.060	1.088	1.167	1.020	1.206
CCDC no.	1989398	2191115	2014911	2191118	2062423	2191117	1989403

Table S3: Structural data (collection at **RT**) and refinement parameters for compounds **1**–**7**.

Compound	1_RT	2_RT	3a_RT	4_RT	5_RT	6_RT	7_RT
Empirical Formula	$C_{13}H_{10}N_2O_4$	$C_{14}H_{14}N_2O_6$	$C_{13}H_9N_2O_3Br$	$C_{13}H_9N_2O_3Cl$	$C_{14}H_9N_2O_3F_3$	$C_{14}H_{12}N_2O_3$	$C_{14}H_{12}N_2O_4$
M. W. (g.mol^{-1})	258.24	306.29	321.13	275.66	310.23	256.26	272.26
T (K)	298	298	298	298	298	298	298
λ (Å)	0.71073	0.71073	0.71073	1.54178	1.54178	0.71073	1.54178
Crystal habit, colour	plate, orange	prism, red-orange	block, orange	needle, yellow	rod, orange	needle, orange	needle, yellow
Crystal size (mm^3)	0.781 x 0.279 x 0.116	0.345 x 0.181 x 0.167	0.533 x 0.264 x 0.222	0.256 x 0.137 x 0.073	0.331 x 0.304 x 0.283	0.260 x 0.219 x 0.084	0.221 x 0.092 x 0.033
Lattice	Monoclinic	Monoclinic	Monoclinic	Monoclinic	Monoclinic	Monoclinic	Monoclinic
Space group	$P2_1/n$	$C2/c$	$P2_1/c$	$P2_1/n$	$C2/m$	$P2_1/c$	$P2_1/n$
a (Å)	6.3334(9)	26.1210(3)	7.5948(12)	14.7430(5)	14.3061(3)	14.0950(6)	3.8838(10)
b (Å)	23.683(3)	7.0281(7)	11.5863(18)	3.7894(10)	6.7681(2)	14.2250(6)	21.6182(5)
c (Å)	7.8211(10)	15.8739(17)	14.0550(2)	21.5528(7)	14.2305(3)	6.2470(3)	15.2697(3)
β (°)	93.769(5)	111.639(4)	94.165(7)	91.845(3)	106.830(2)	95.355(17)	96.652(2)
Vol (Å^3)	1170.6(3)	2708.8(5)	1233.5(3)	1203.47(6)	1318.85(6)	1247.2(9)	1273.43(5)
Z	4	8	4	4	4	4	4
D_{calcd} (g.cm^{-3})	1.465	1.424	1.729	1.521	1.557	1.375	1.420
F(000)	536.0	1216	640.0	564.0	628.0	536	570.1
μ (mm^{-1})	0.111	0.110	3.446	2.882	1.218	0.098	0.888
No. reflns	23657	14279	32288	6431	8627	34150	17323
Data / restr. / par.	1186 / 0 / 182	1506 / 0 / 198	3075 / 0 / 173	2461 / 0 / 173	1262 / 44 / 140	1534 / 0 / 179	2284 / 0 / 185
R(int) / R(sigma)	0.1021 / 0.0281	0.1243 / 0.0468	0.0395 / 0.0235	0.0234 / 0.0292	0.0199 / 0.0106	0.0944 / 0.0223	0.0337 / 0.0149
R_1 / wR_2 ($I > 2\sigma(I)$)[a]	0.0885 / 0.2445	0.0572 / 0.1502	0.0325 / 0.0746	0.0395 / 0.1063	0.0510 / 0.1437	0.0658 / 0.1542	0.0364 / 0.1045
R_1 / wR_2 [all data]	0.1486 / 0.3586	0.1247 / 0.2331	0.0543 / 0.0856	0.0503 / 0.1159	0.0561 / 0.1470	0.1238 / 0.2363	0.0386 / 0.1072
GOOF	1.198	1.058	1.037	1.047	1.139	0.860	1.106
CCDC no.	2191114	2191116	1966932	2156467	1989369	2191119	2049690

Table S4: Crystallographic details of compound **3b** from 150–300 K

Compound	**3b_150K**	**3b_180K**	**3b_210K**	**3b_240K**	**3b_270K**	**3b_300K**
Empirical Formula	$C_{13}H_9N_2O_3Br$	$C_{13}H_9N_2O_3Br$	$C_{13}H_9N_2O_3Br$	$C_{13}H_9N_2O_3Br$	$C_{13}H_9N_2O_3Br$	$C_{13}H_9N_2O_3Br$
M. W. ($g.mol^{-1}$)	321.12	321.12	321.12	321.12	321.12	321.12
T (K)	150	180	210	240	270	300
λ (Å)	1.54178	1.54178	1.54178	1.54178	1.54178	1.54178
Crystal habit, colour	block, orange-brown	block, orange-brown	block, orange-brown	block, orange-brown	block, orange-brown	block, orange-brown
Crystal size (mm^3)	0.716 x 0.237 x 0.186	0.716 x 0.237 x 0.186	0.716 x 0.237 x 0.186	0.716 x 0.237 x 0.186	0.716 x 0.237 x 0.186	0.716 x 0.237 x 0.186
Lattice	Monoclinic	Monoclinic	Monoclinic	Monoclinic	Monoclinic	Monoclinic
Space group	$P2_1/c$	$P2_1/c$	$P2_1/c$	$P2_1/c$	$P2_1/c$	$P2_1/c$
a (Å)	7.4403(10)	7.4688(10)	7.4982(10)	7.5309(10)	7.5635(2)	7.5995(10)
b (Å)	11.5220(2)	11.5368(2)	11.5476(2)	11.5580(2)	11.5743(3)	11.5868(2)
c (Å)	14.0179(2)	14.0272(2)	14.0374(2)	14.0459(2)	14.0536(3)	14.0731(2)
β (°)	93.6690(10)	93.764(10)	93.869(10)	94.004(10)	94.109(2)	94.2470(10)
Vol ($Å^3$)	1199.25(3)	1206.06(3)	1212.68(3)	1219.60(3)	1227.12(5)	1235.79(3)
Z	4	4	4	4	4	4
D_{calcd} ($g.cm^{-3}$)	1.773	1.763	1.753	1.743	1.733	1.721
F(000)	599.0	636.0	636.0	636.0	636.0	636.0
μ (mm^{-1})	4.747	4.720	4.694	4.668	4.639	4.607
No. reflns	14931	14426	15147	14419	8199	15577
Data / restr. / par.	2522 / 0 / 173	2529/ 0 / 173	2542 / 0 / 172	2564 / 0 / 173	2530 / 0 / 173	2596 / 0 / 173
R(int) / R(sigma)	0.0318 / 0.0156	0.0579 / 0.0263	0.0341 / 0.0162	0.0690 / 0.0286	0.0268/ 0.0223	0.0552 / 0.0256
R_1 / wR_2 ($I > 2\sigma(I)$)[a]	0.0256 / 0.0677	0.0369 / 0.1023	0.0314 / 0.0870	0.0378 / 0.1017	0.0349 / 0.0936	0.0367 / 0.1027
R_1 / wR_2 [all data]	0.0265 / 0.0683	0.0384 / 0.1034	0.0329/ 0.0881	0.0403 / 0.1033	0.0385 / 0.0964	0.0388 / 0.1046
GOOF	1.037	1.085	1.091	1.048	1.055	1.077
CCDC No.	2156456	2156457	2156458	2156459	2156460	2156461

Table S5: Crystallographic details of compound **4** from 150–300 K

Compound	**4_150K**	**4_180K**	**4_210K**	**4_240K**	**4_270K**	**4_300K**
Empirical Formula	$C_{13}H_9N_2O_3Cl$	$C_{13}H_9N_2O_3Cl$	$C_{13}H_9N_2O_3Cl$	$C_{13}H_9N_2O_3Cl$	$C_{13}H_9N_2O_3Cl$	$C_{13}H_9N_2O_3Cl$
M. W. ($g.mol^{-1}$)	275.66	275.66	275.66	275.66	275.66	275.66
T (K)	150	180	210	240	270	300
λ (Å)	1.54178	1.54178	1.54178	1.54178	1.54178	1.54178
Crystal habit, colour	needle, yellow	needle, yellow	needle, yellow	needle, yellow	needle, yellow	needle, yellow
Crystal size (mm^3)	0.256 x 0.137 x 0.073	0.256 x 0.137 x 0.073	0.256 x 0.137 x 0.073	0.256 x 0.137 x 0.073	0.256 x 0.137 x 0.073	0.256 x 0.137 x 0.073
Lattice	Monoclinic	Monoclinic	Monoclinic	Monoclinic	Monoclinic	Monoclinic
Space group	$P2_1/n$	$P2_1/n$	$P2_1/n$	$P2_1/n$	$P2_1/n$	$P2_1/n$
a (Å)	14.6564(3)	14.6708(2)	14.6907(2)	14.7034(3)	14.7251(3)	14.7430(5)
b (Å)	3.7374(1)	3.7471(10)	3.7572(5)	3.7661(10)	3.7787(10)	3.7894(10)
c (Å)	21.4431(4)	21.4612(3)	21.4853(3)	21.5036(4)	21.5304(3)	21.5528(7)
β (°)	92.109(2)	92.028(2)	91.9844(13)	91.9240(2)	91.869(2)	91.845(3)
Vol ($Å^3$)	1173.80(5)	1179.05(4)	1185.20(3)	1190.08(5)	1197.35(4)	1203.47(6)
Z	4	4	4	4	4	4
D_{calcd} ($g.cm^{-3}$)	1.560	1.553	1.545	1.539	1.539	1.521
F(000)	564.0	564.0	564.0	564.0	564.0	564.0
μ (mm^{-1})	2.955	2.942	2.927	2.915	2.897	2.882
No. reflns	11919	12250	12380	12317	12528	6431
Data / restr. / par.	2249 / 0 / 176	2475 / 0 / 173	2484 / 0 / 173	2507 / 0 / 173	2503 / 0 / 172	2461 / 0 / 173
R(int) / R(sigma)	0.0556 / 0.0308	0.0390 / 0.0252	0.0321 / 0.0221	0.0364 / 0.0228	0.0345 / 0.0240	0.0234 / 0.0292
R_1 / wR_2 ($I > 2\sigma(I)$)[a]	0.0437 / 0.1234	0.0366 / 0.1006	0.0352 / 0.0929	0.0362 / 0.1003	0.0407 / 0.1217	0.0395 / 0.1063
R_1 / wR_2 [all data]	0.0468/ 0.1264	0.0396/ 0.1030	0.0389/ 0.0956	0.0416/ 0.1045	0.0461/ 0.1263	0.0503 / 0.1159
GOOF	1.088	1.078	1.074	1.080	1.062	1.047
CCDC No.	2156462	2156463	2156464	2156465	2156466	2156467

Table S6: Crystallographic details of compound **5** from 150–300 K

Compound	**5_150K**	**5_180K**	**5_210K**	**5_240K**	**5_270K**	**5_300K**
Empirical Formula	$C_{14}H_9F_3N_2O_3$	$C_{14}H_9F_3N_2O_3$	$C_{14}H_9F_3N_2O_3$	$C_{14}H_9F_3N_2O_3$	$C_{14}H_9F_3N_2O_3$	$C_{14}H_9F_3N_2O_3$
M. W. ($g.mol^{-1}$)	309.22	309.22	309.22	309.22	309.22	309.22
T (K)	150	180	210	240	270	300
λ (Å)	1.54178	1.54178	1.54178	1.54178	1.54178	1.54178
Crystal habit, colour	plate, orange	plate, orange	plate, orange	plate, orange	plate, orange	plate, orange
Crystal size (mm^3)	0.343 x 0.284 x 0.212	0.343 x 0.284 x 0.212	0.343 x 0.284 x 0.212	0.343 x 0.284 x 0.212	0.343 x 0.284 x 0.212	0.343 x 0.284 x 0.212
Lattice	Monoclinic	Monoclinic	Monoclinic	Monoclinic	Monoclinic	Monoclinic
Space group	*C*2/*m*	*C*2/*m*	*C*2/*m*	*C*2/*m*	*C*2/*m*	*C*2/*m*
a (Å)	14.3165(4)	14.3145(4)	14.3133(3)	14.3118(4)	14.3128(6)	14.3168(6)
b (Å)	6.59390(2)	6.62200(2)	6.6574(10)	6.69250(2)	6.73270(2)	6.77160(3)
c (Å)	14.1523(3)	14.1681(4)	14.1840(3)	14.1987(3)	14.2071(5)	14.2320(5)
β (°)	107.224(3)	107.166(3)	107.075(2)	106.993(3)	107.952(4)	106.790(4)
Vol ($Å^3$)	1276.09(7)	1283.18(7)	1292.01(5)	1300.60(6)	1309.56(9)	1320.94(10)
Z	4	4	4	4	4	4
D_{calcd} ($g.cm^{-3}$)	1.610	1.601	1.590	1.579	1.568	1.555
F(000)	628.0	628.0	628.0	628.0	628.0	628.0
μ (mm^{-1})	1.259	1.252	1.243	1.235	1.227	1.216
No. reflns	6528	6866	6927	6938	6685	6419
Data / restr. / par.	1442 / 0 / 133	1447 / 0 / 133	1461 / 0 / 133	1483 / 0 / 133	1476 / 0 / 133	1460 / 0 / 133
R(int) / R(sigma)	0.0304 / 0.0166	0.0267 / 0.0150	0.0243 / 0.0137	0.0280 / 0.0153	0.0325 / 0.0176	0.0623 / 0.0304
R_1 / wR_2 ($I > 2\sigma(I)$)[a]	0.0403 / 0.1185	0.0403 / 0.1224	0.0428 / 0.1372	0.0560 / 0.1475	0.0640 / 0.1574	0.0655 / 0.2135
R_1 / wR_2 [all data]	0.0460 / 0.1205	0.0438 / 0.1241	0.0479 / 0.1397	0.0616 / 0.1495	0.0763 / 0.1616	0.0728 / 0.2377
GOOF	1.208	1.162	1.204	1.214	1.261	1.183
CCDC No.	2191108	2191109	2191110	2191111	2191112	2191113

Table S7: Crystallographic details of compounds **1**, **2**, **5** and **6** at different temperatures in Kelvin.

Compound	1_200K	2_100K	2_200K	5_140K	6_200K	6_230K
Empirical Formula	$C_{13}H_{10}N_2O_4$	$C_{14}H_{14}N_2O_6$	$C_{14}H_{14}N_2O_6$	$C_{14}H_9F_3N_2O_3$	$C_{14}H_{12}N_2O_3$	$C_{14}H_{12}N_2O_3$
M. W. ($g.mol^{-1}$)	258.24	306.29	306.29	309.22	256.26	256.26
T (K)	200	100	200	140	200	230
λ (Å)	0.71073	0.71073	0.71073	1.54178	0.71073	0.71073
Crystal habit, colour	plate, orange	plate, yellow	plate, brown	plate, orange	block, orange	block, orange
Crystal size (mm^3)	0.781 x 0.279 x 0.116	0.272 x 0.076 x 0.031	0.672 x 0.623 x 0.030	0.331 x 0.304 x 0.283	0.492 x 0.491 x 0.164	0.772 x 0.668 x 0.120
Lattice	Monoclinic	Monoclinic	Monoclinic	Monoclinic	Monoclinic	Monoclinic
Space group	$P2_1/n$	$C2/c$	$C2/c$	$C2/m$	$P2_1/c$	$P2_1/c$
a (Å)	6.2976(4)	26.0205(13)	26.0764(13)	14.3244(3)	14.0746(5)	14.0772(11)
b (Å)	23.6484(13)	6.8984(4)	6.9741(4)	6.5885(10)	14.0175(6)	14.1814(12)
c (Å)	7.7663(4)	15.7463(8)	15.7872(7)	14.1537(3)	6.1991(3)	6.2335(5)
β (°)	94.638(2)	111.802(2)	111.460(2)	107.249(2)	95.245(2)	95.379(4)
Vol ($Å^3$)	1152.83(11)	2624.3(2)	2672.0(2)	1275.70(4)	1217.9(9)	1238.94(17)
Z	4	8	8	4	4	4
D_{calcd} ($g.cm^{-3}$)	1.488	1.467	1.433	1.610	1.3975	1.374
F(000)	536.0	1213.5	1216.7	628.0	536.3	536.3
μ (mm^{-1})	0.113	0.113	0.111	1.259	0.100	0.099
No. reflns	21349	17663	22631	6765	22992	31233
Data / restr. / par.	2819 / 0 / 175	3208 / 0 / 199	2375 / 0 / 197	1456 / 0 / 133	3013 / 0 / 181	3037 / 0 / 176
R(int) / R(sigma)	0.0256 / 0.0181	0.0734 / 0.0505	0.0301 / 0.0227	0.0297 / 0.0173	0.0239 / 0.0165	0.0455 / 0.0247
R_1 / wR_2 ($I > 2\sigma(I)$)[a]	0.0426 / 0.0997	0.0418 / 0.0994	0.0410 / 0.1010	0.0403 / 0.1173	0.0426 / 0.1281	0.0494 / 0.1325
R_1 / wR_2 [all data]	0.0503 / 0.1083	0.0628 / 0.1194	0.0650 / 0.1149	0.0447 / 0.1195	0.0524 / 0.1260	0.0666 / 0.1598
GOOF	1.061	1.092	1.028	1.112	1.070	1.141
CCDC No.	1899401	2014914	2049691	2191107	1902658	2019418

5. Calculation of Thermal Expansion Coefficient by *PASCal*[3] Program

Table S8: Thermal Expansion Coefficient of compounds **3b**, **4** and **5** within the temperature range of 150 K to 300 K

Compound 3b			**Direction**		
Axes	**α(MK^{-1})**	**σα(MK^{-1})**	**a**	**b**	**c**
X1	12.9993	1.4643	0.5000	0.0000	1.0000
X2	34.6335	2.3045	0.0000	1.0000	0.0000
X3	149.3944	3.1099	1.0000	0.0000	0.0000
V	199.2712	6.4910			
Compound 4			**Direction**		
Axes	**α(MK^{-1})**	**σα(MK^{-1})**	**a**	**b**	**c**
X1	21.7624	1.6850	1.0000	0.0000	1.0000
X2	53.2469	0.6224	1.0000	0.0000	0.5000
X3	92.6797	1.4683	0.0000	-1.0000	0.0000
V	169.3825	2.8789			
Compound 5			**Direction**		
Axes	**α(MK^{-1})**	**σα(MK^{-1})**	**a**	**b**	**c**
X1	-6.4204	0.3494	1.0000	0.0000	0.0000
X2	56.5010	3.7664	0.5000	0.0000	1.0000
X3	181.365	4.7626	0.0000	1.0000	0.0000
V	233.9546	8.0894			

6. Fourier-transform Infrared (IR) Absorption Spectroscopy

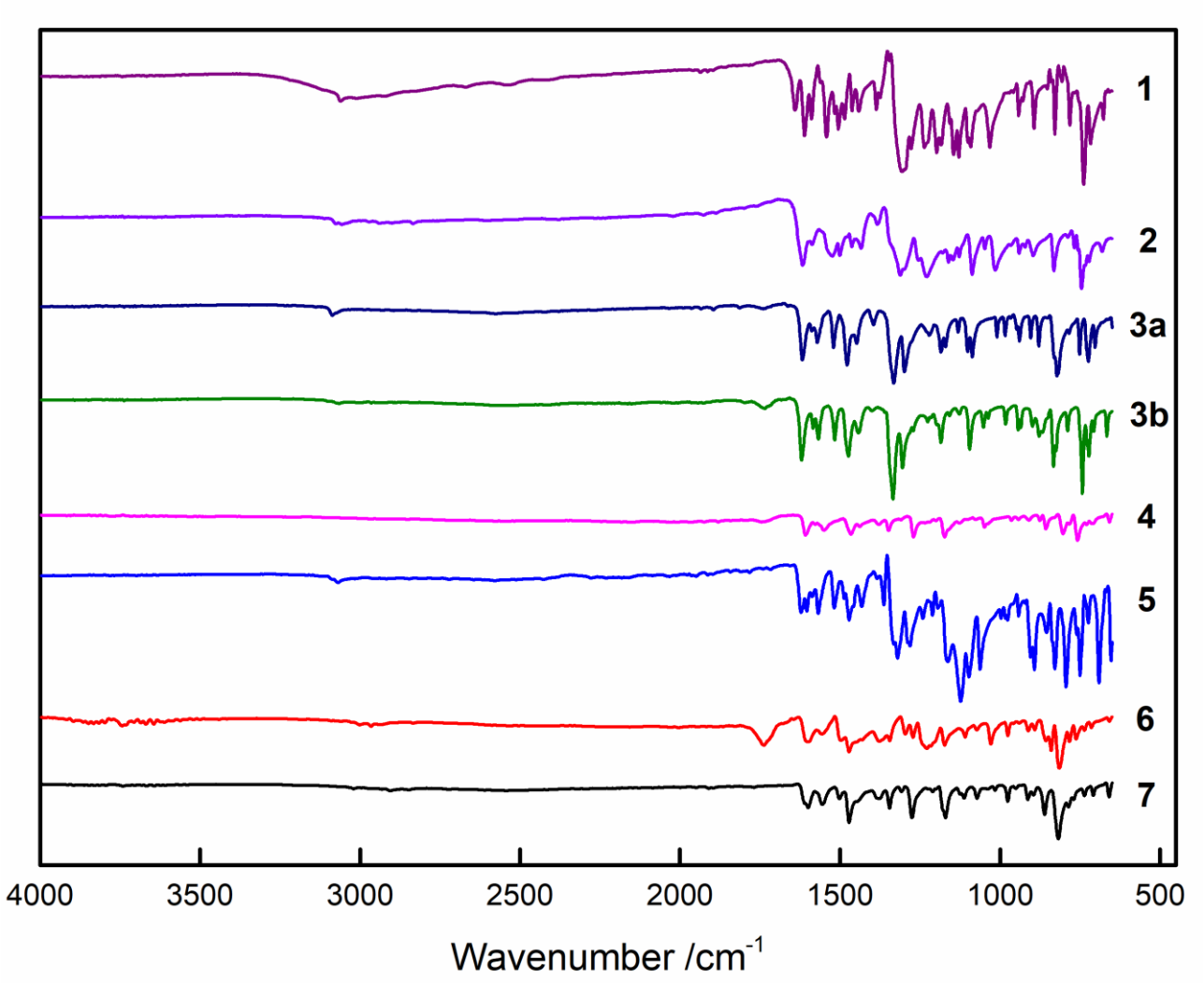

Figure 6. Fourier-transform infrared (IR) spectra for compounds **1**–**7**.

7. Liquid-State ^{1}H, ^{13}C Nuclear Magnetic Resonance (NMR) Spectroscopy

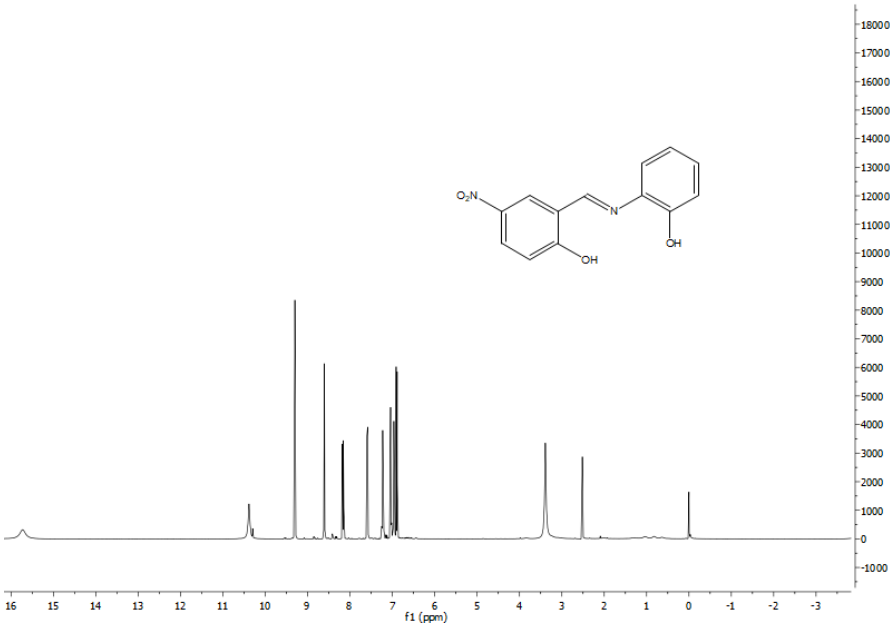

Figure 7(a). Liquid-state ^{1}H NMR spectrum of compound **1** in DMSO-d_6 at 298 K.

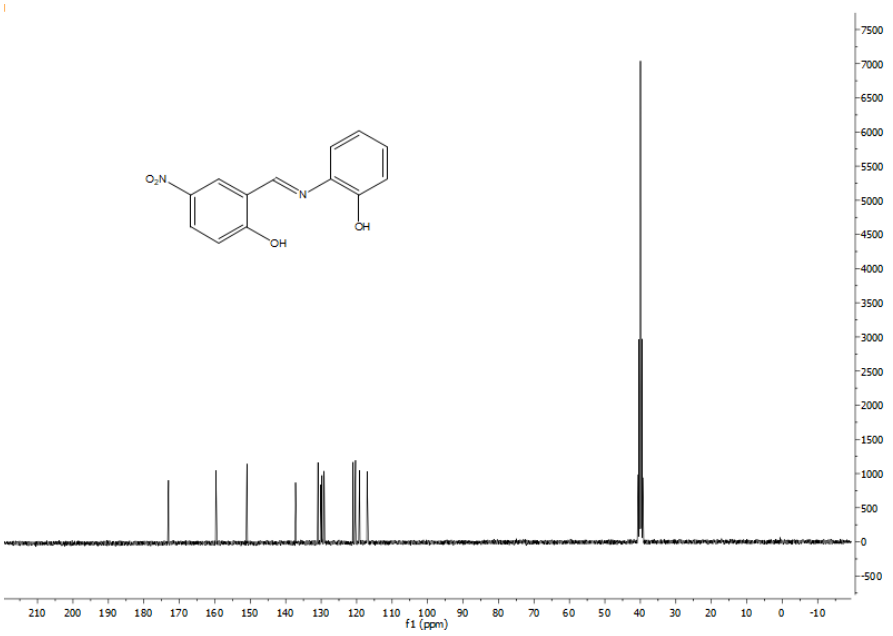

Figure 7(b). Liquid-state ^{13}C NMR spectrum of compound **1** in DMSO-d_6 at 298 K.

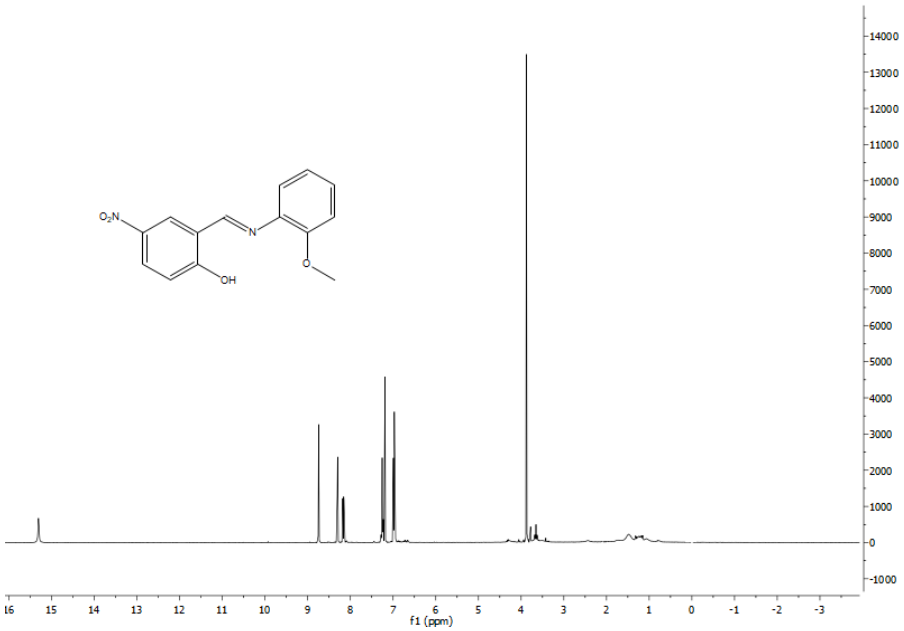

Figure S7(c). Liquid-state ^{1}H NMR spectrum of compound **2** in $CDCl_3$ at 298 K.

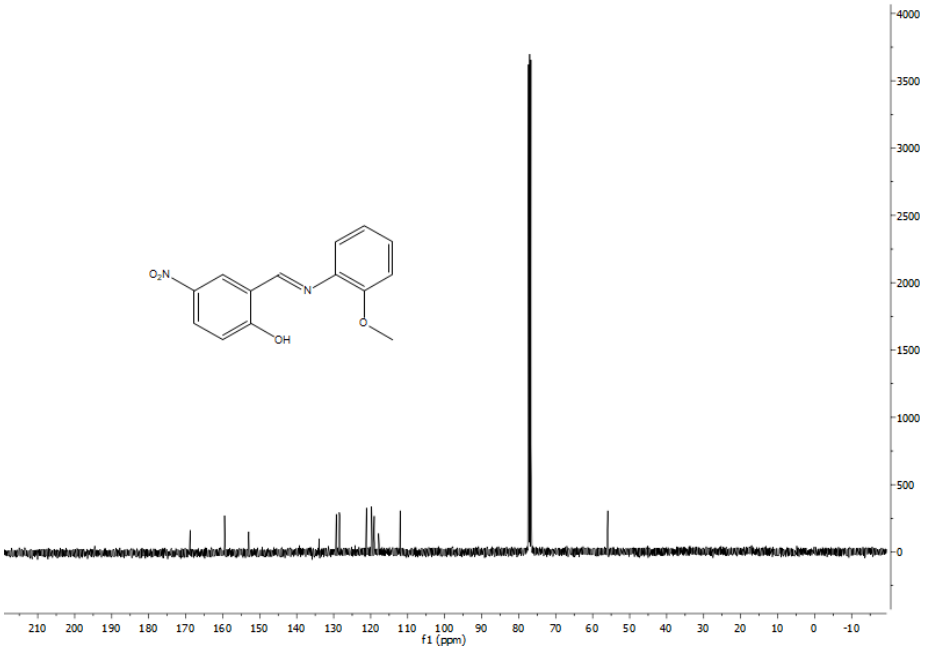

Figure S7(d). Liquid-state ^{13}C NMR spectrum of compound **2** in $CDCl_3$ at 298 K.

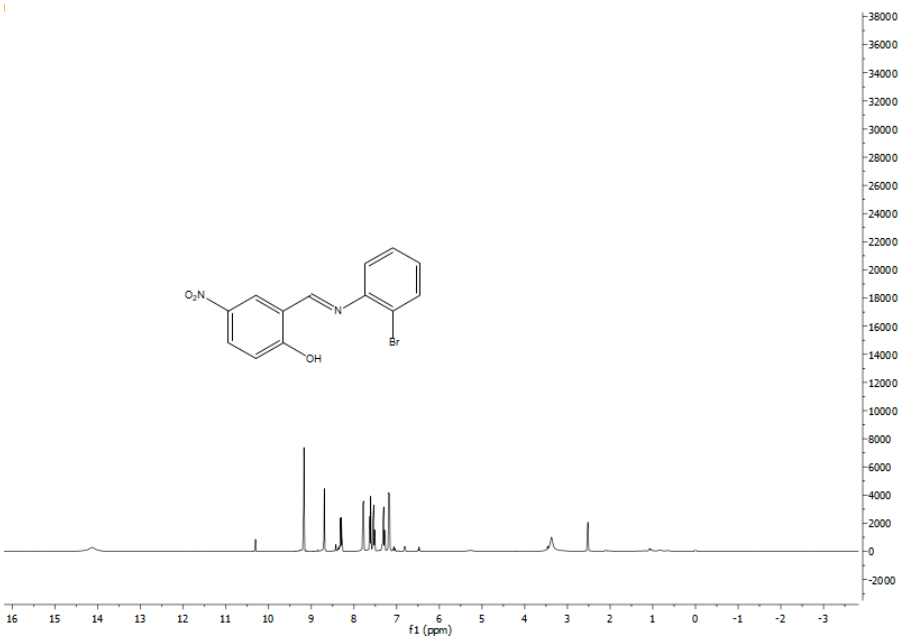

Figure S7(e). Liquid-state ^{1}H NMR spectrum of compound **3b** in $CDCl_3$ at 298 K.

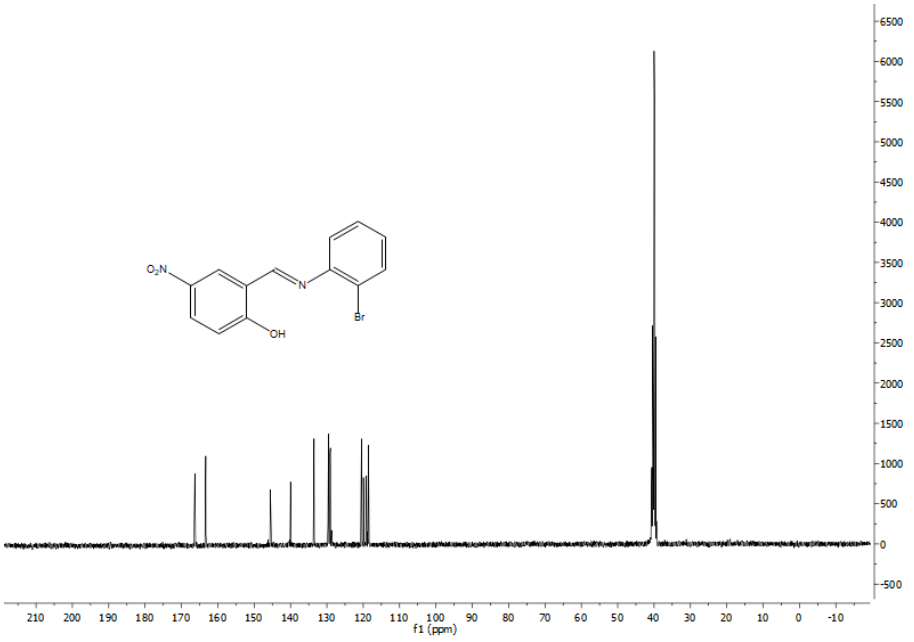

Figure S7(f). Liquid-state ^{13}C NMR spectrum of compound **3b** in DMSO-d_6 at 298 K.

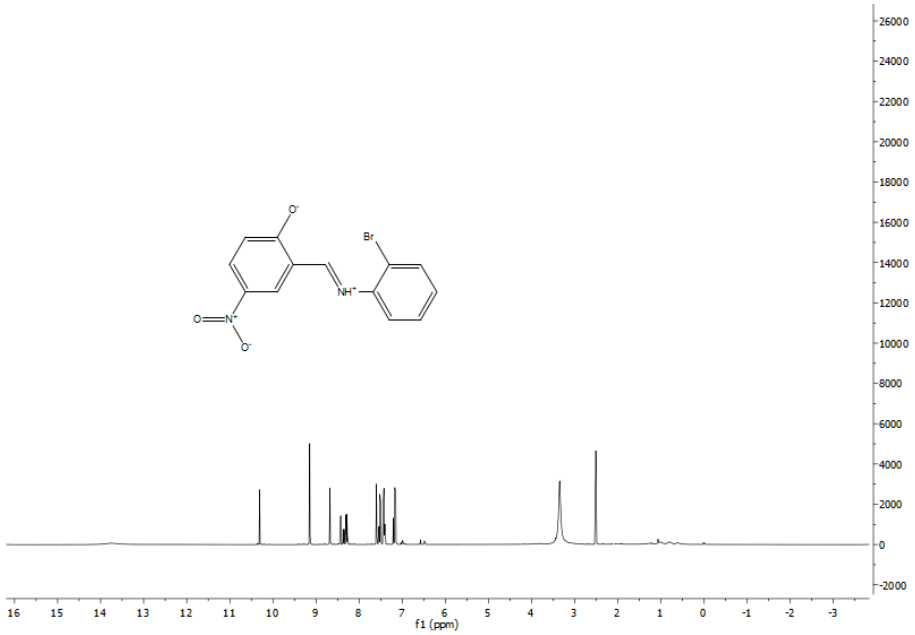

Figure S7(g). Liquid-state ^{1}H NMR spectrum of compound **3a** in $CDCl_3$ at 298 K.

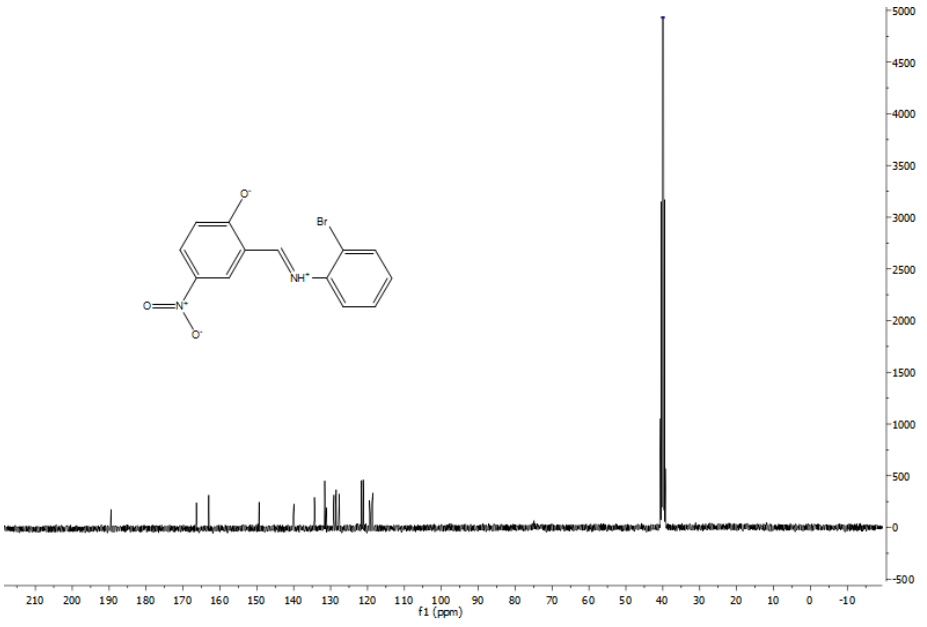

Figure S7(h). Liquid-state ^{13}C NMR spectrum of compound **3a** in DMSO-d_6 at 298 K.

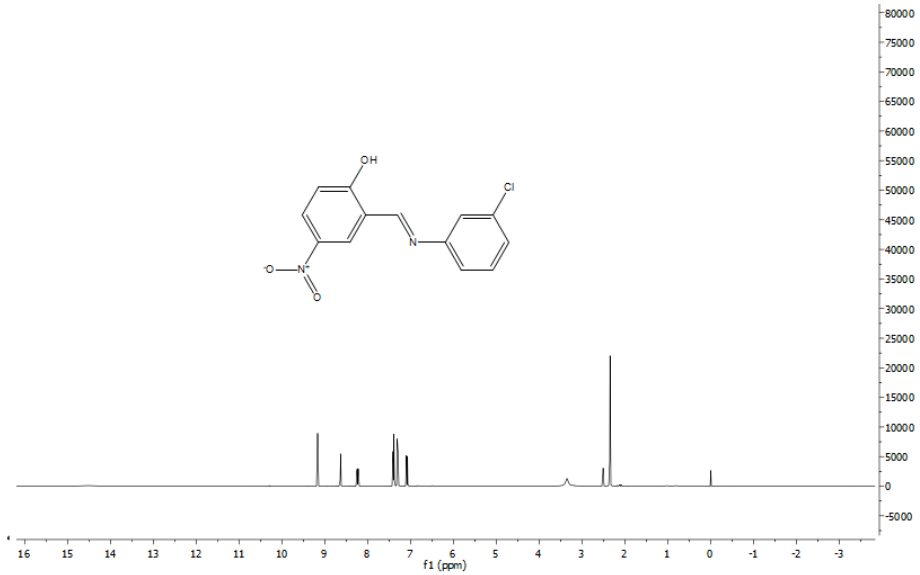

Figure S7(i). Liquid-state ^{1}H NMR spectrum of compound **4** in $CDCl_3$ at 298 K.

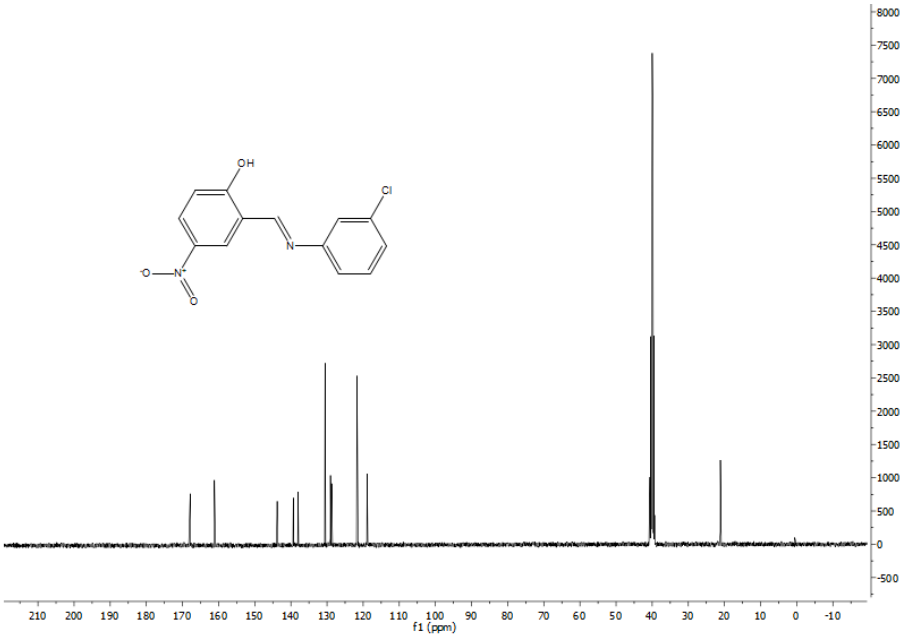

Figure S7(j). Liquid-state ^{13}C NMR spectrum of compound **4** in $CDCl_3$ at 298 K.

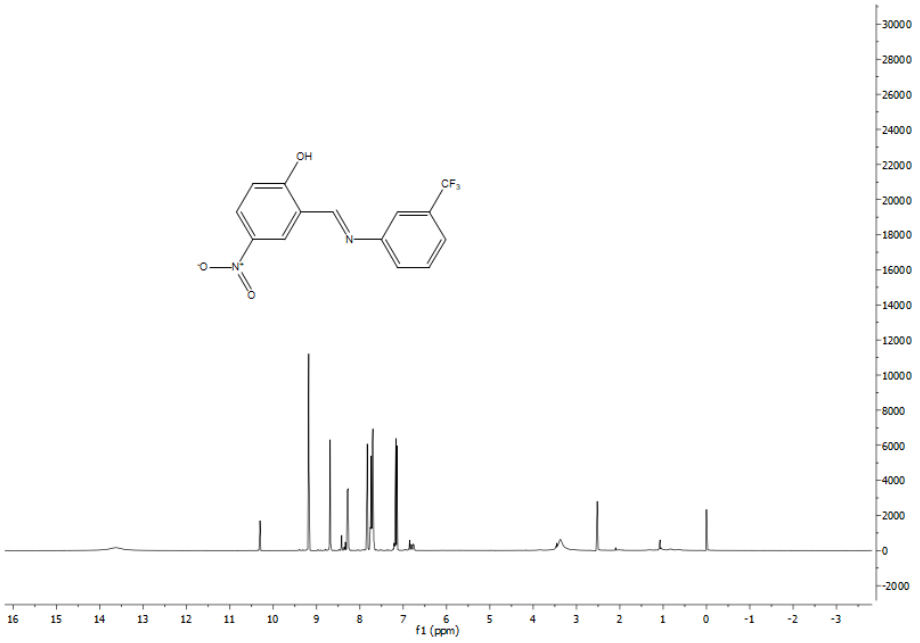

Figure S7(k). Liquid-state ^{1}H NMR spectrum of compound **5** in DMSO-d_6 at 298 K.

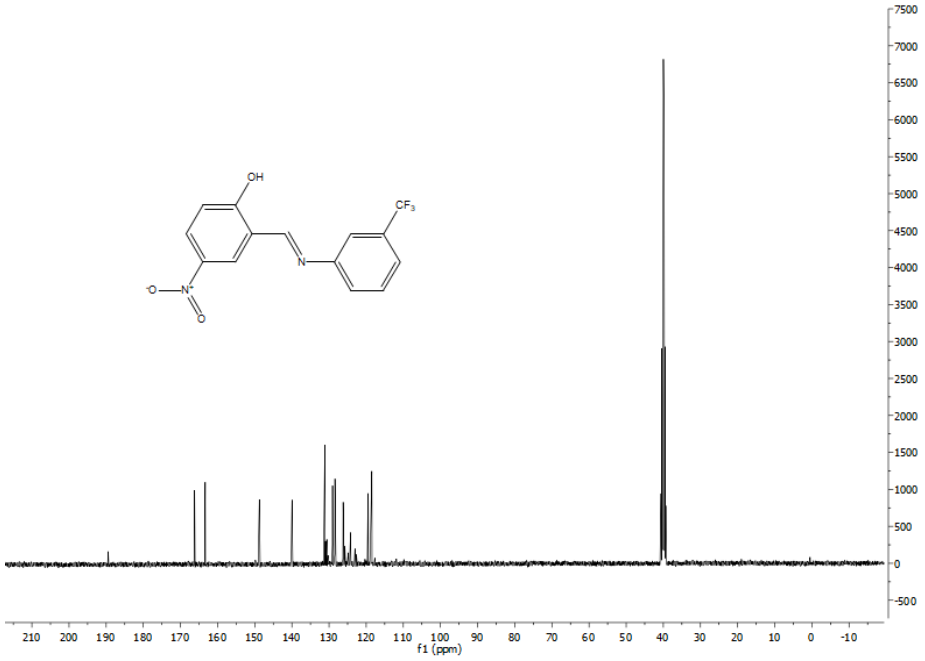

Figure S7(l). Liquid-state ^{13}C NMR spectrum of compound **5** in DMSO-d_6 at 298 K.

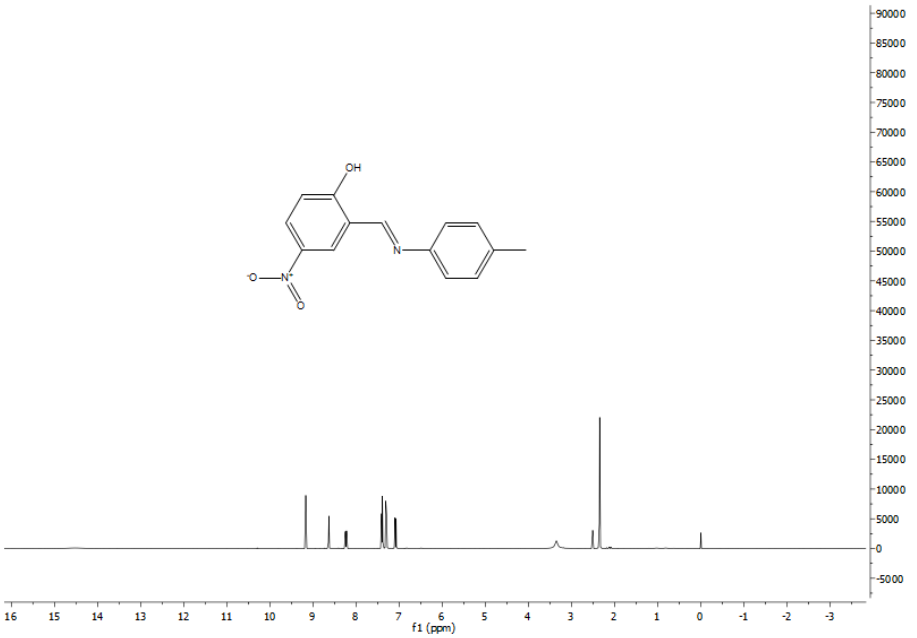

Figure S7(m). Liquid-state ^{1}H NMR spectrum of compound **6** in $CDCl_3$ at 298 K.

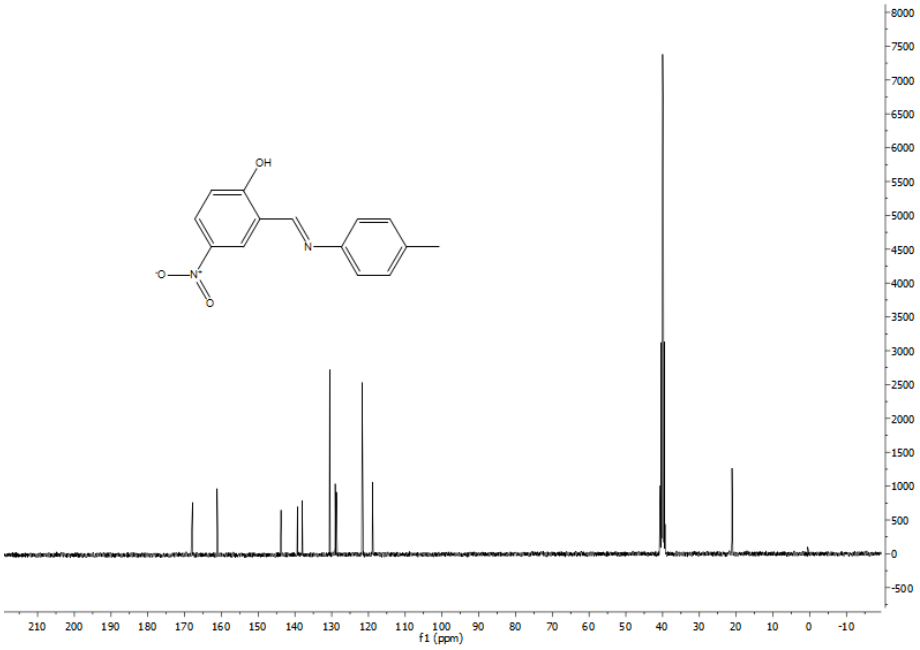

Figure S7(n). Liquid-state ^{13}C NMR spectrum of compound **6** in DMSO-d_6 at 298 K.

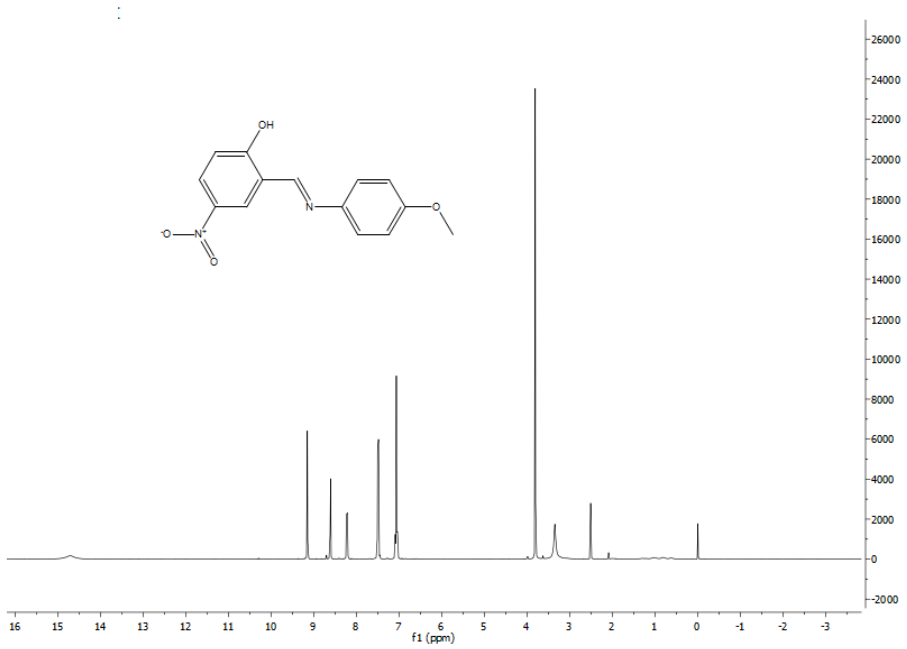

Figure S7(o) Liquid-state ^{1}H NMR spectrum of compound **7** in DMSO-d_6 at 298 K.

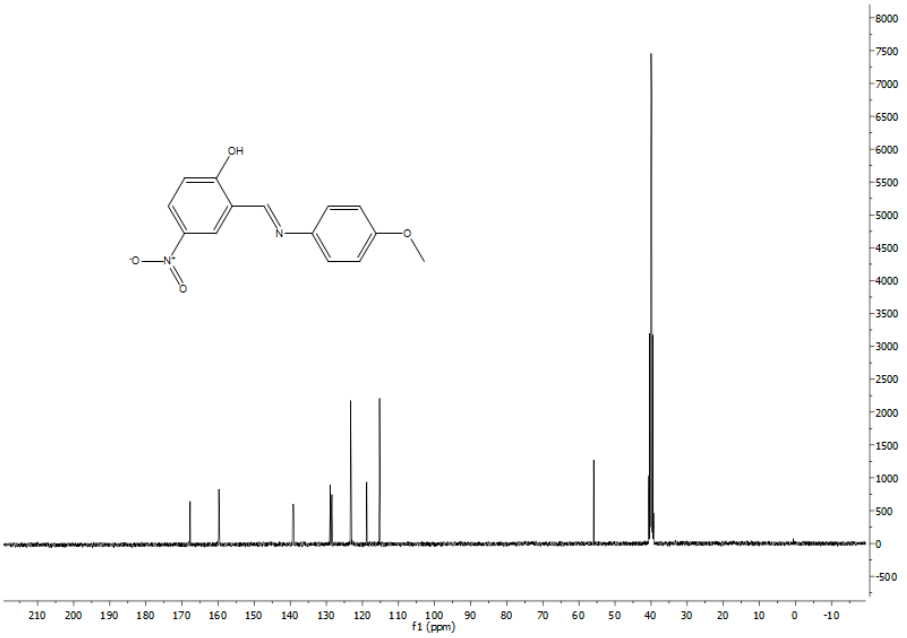

Figure S7(p) Liquid-state ^{13}C NMR spectrum of compound **7** in DMSO-d_6 at 298 K.

8. Mass Spectroscopy

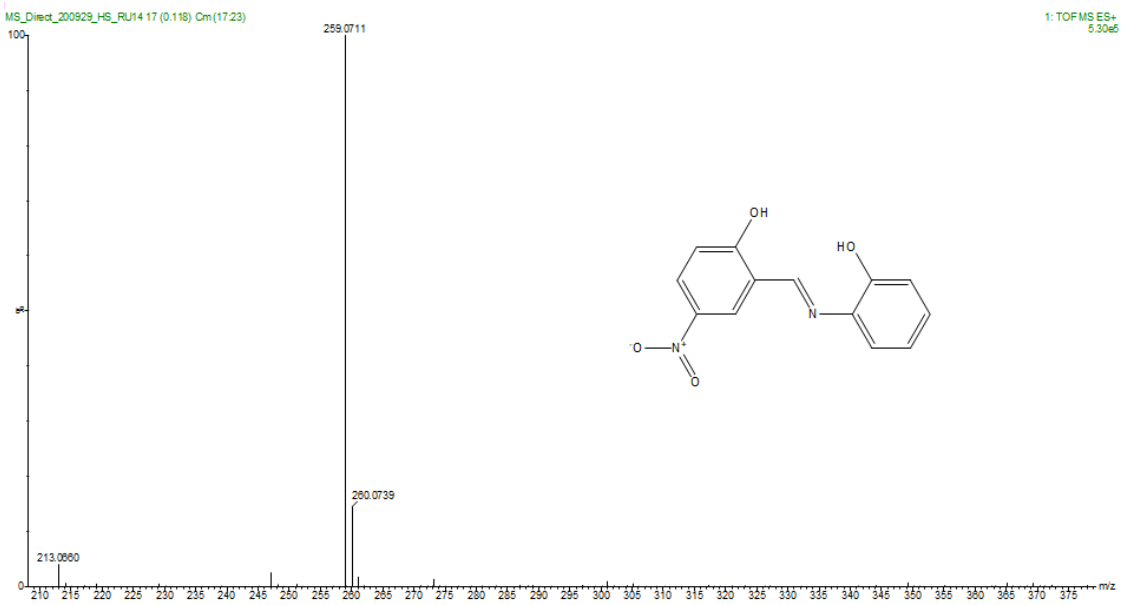

Figure S8(a). Mass spectrum (MS) for compound **1.**

Figure S8(b). Mass spectrum (MS) for compound **2**.

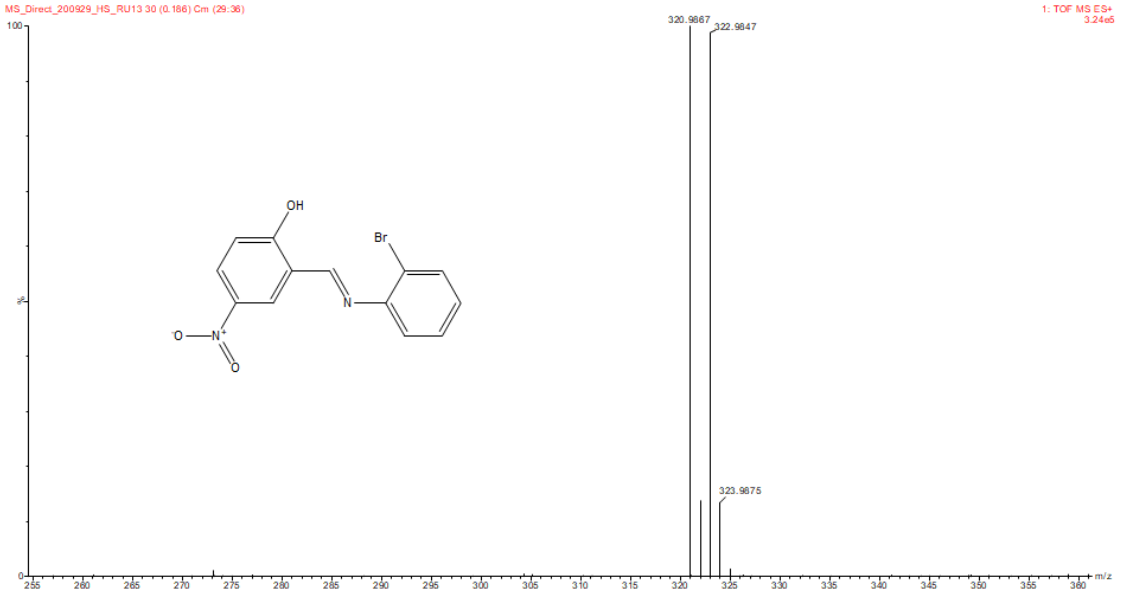

Figure S8(c). Mass spectrum (MS) for compound **3b**.

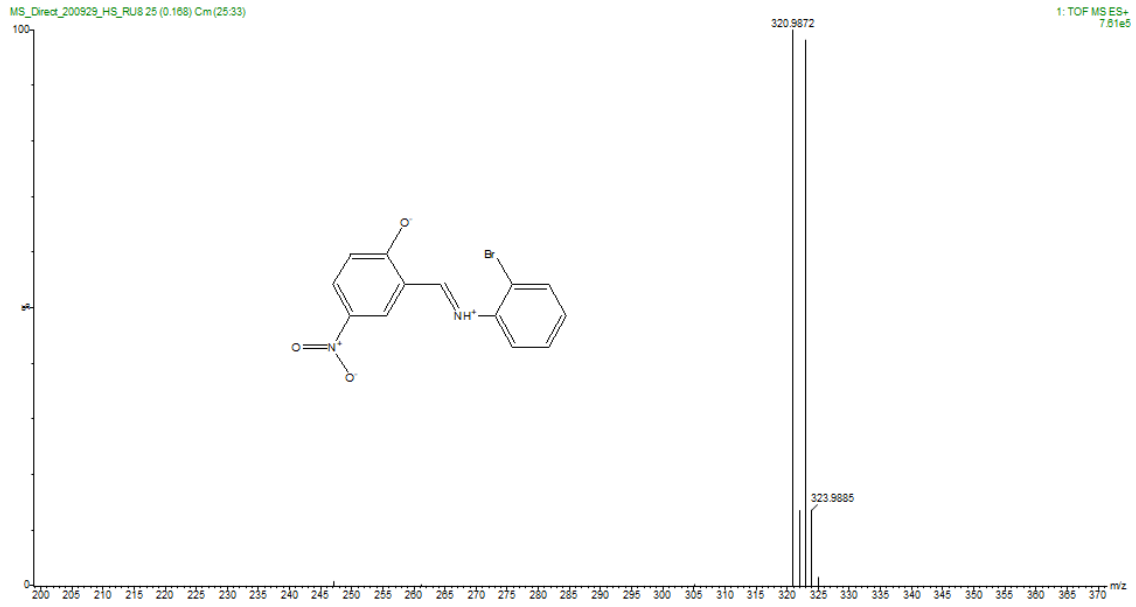

Figure S8(d). Mass spectrum (MS) for compound **3a**.

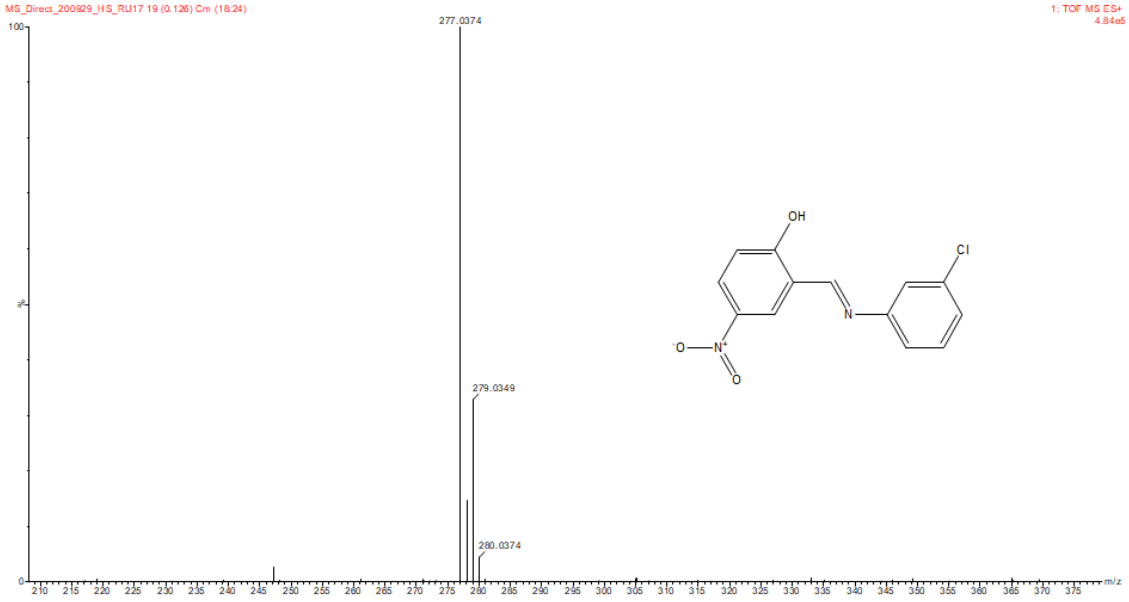

Figure S8(e). Mass spectrum (MS) for compound **4**.

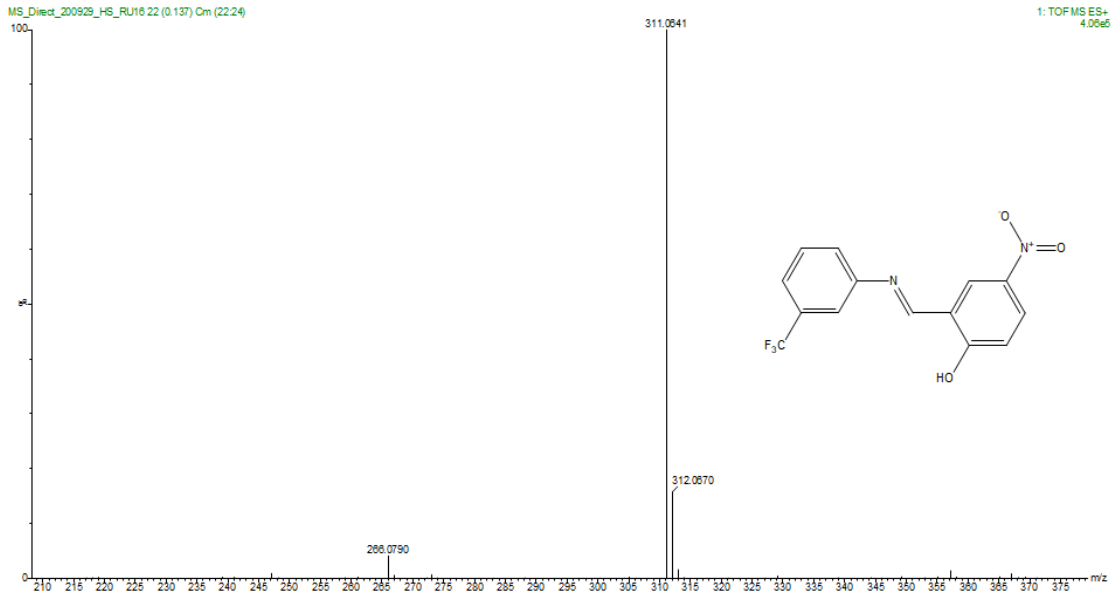

Figure S8(f). Mass spectrum (MS) for compound **5**.

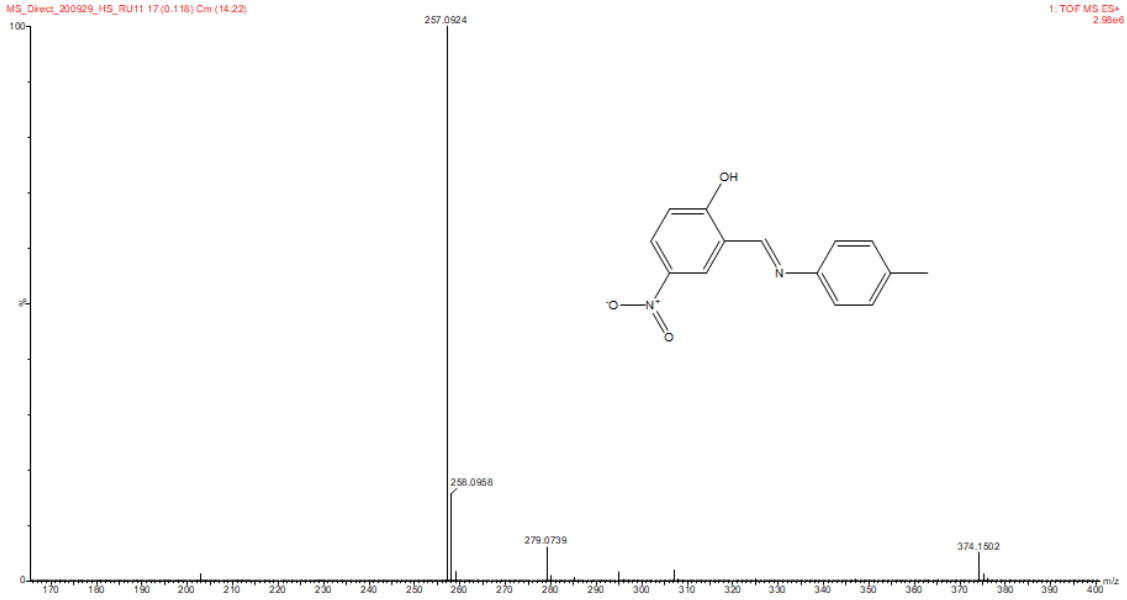

Figure S8(g). Mass spectrum (MS) for compound **6**.

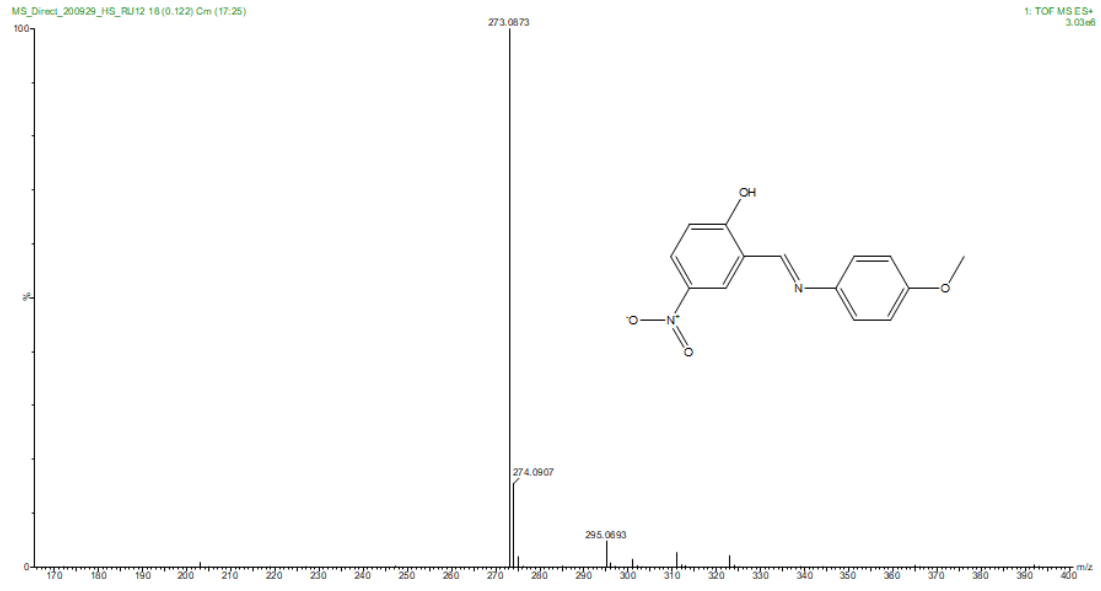

Figure S8(h). Mass spectrum (MS) for compound **7**.

9. Solid-State Absorption Ultraviolet Visible Spectroscopy

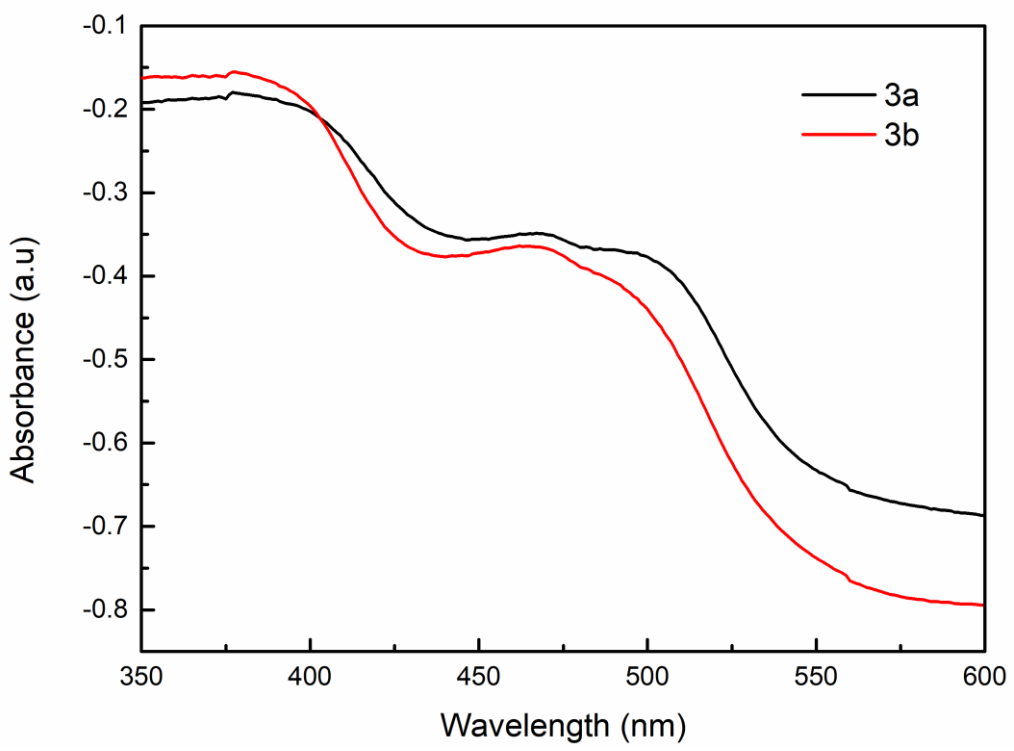

Figure S9. Solid-state ultraviolet-visible spectra for compounds **3a** and **3b**.

10. Differential Scanning Calorimetry (DSC) Measurements

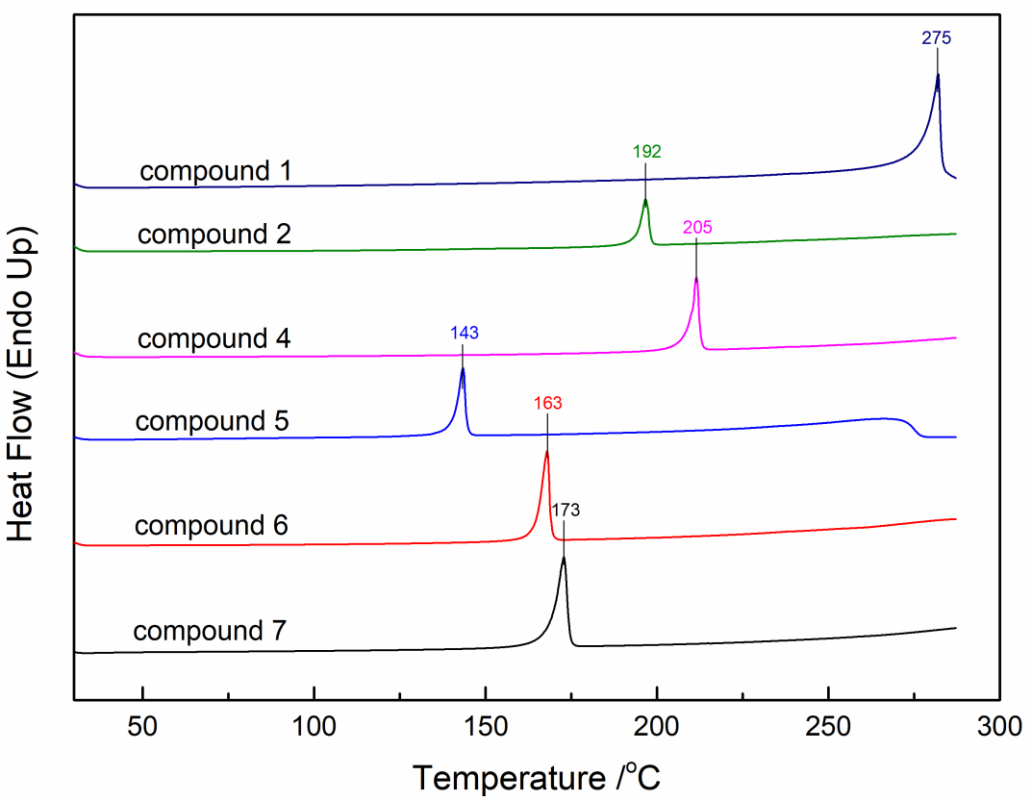

Figure S10(a). DSC curves (Endotherm Up and Exotherm Down) showing melting points of compounds **1** (275 °C or 573 K), **2** (192 °C or 490 K), **4** (205 °C or 503 K), **5** (143 °C or 441 K), **6** (163 °C or 461 K) and **7** (173 °C or 471 K).

11. References

1. A. L. Spek, PLATON, molecular geometry program, *J. Appl. Crystallogr*. 2003, **36**, 7–13.
2. C. F. Macrae, I. J. Bruno, J. A. Chisholm, P. R. Edgington, P. McCabe, E. Pidcock, L. Rodriguez-Monge, R. Taylor, J. van de Streek, P. A. Wood, *J. Appl. Crystallogr*. 2008, **41**, 466–470.
3. M. J. Cliffe, A. L. Goodwin, *PASCal*: A Principal Axis Strain Calculator for Thermal Expansion and Compressibility Determination. *J. Appl. Crystallogr*, 2012, **45**, 1321–1329.